A New N-Terminal Recognition Domain in Caveolin-1 Interacts with Sterol Carrier Protein-2 (SCP-2) †

ARTICLE *in* BIOCHEMISTRY · AUGUST 2007

Impact Factor: 3.02 · DOI: 10.1021/bi7002636 · Source: PubMed

Published in final edited form as:
Biochemistry. 2007 July 17; 46(28): 8301–8314. doi:10.1021/bi7002636.

A New N-terminal Recognition Domain in Caveolin-1 Interacts with Sterol Carrier Protein-2 (SCP-2)†

Rebecca D. Parr[§], **Gregory G. Martin**[⊥], **Heather A. Hostetler**[⊥], **Megan E. Schroeder**[§], **Kiran D. Mir**[§,‖], **Ann B. Kier**[§], **Judith M. Ball**[*,§], and **Friedhelm Schroeder**[⊥]
[§]Department of Pathobiology, Texas A&M University, TVMC, College Station, TX77843-4467

[⊥]Department of Physiology and Pharmacology, Texas A&M University, TVMC, College Station, TX77843-4466

Abstract

Although plasma membrane domains such as caveolae provide an organizing principle for signaling pathways and cholesterol homeostasis in the cell, relatively little is known regarding specific mechanisms whereby intracellular lipid binding proteins are targeted to caveolae. Therefore, the interaction between caveolin-1 and sterol carrier protein-2 (SCP-2), a protein that binds and transfers both cholesterol and signaling lipids (e.g. phosphatidylinositides, sphingolipids), was examined by yeast two-hybrid, *in vitro* binding, and fluorescence resonance energy transfer analyses (FRET). Results of the *in vivo* and *in vitro* assays identified for the first time the N-terminal aa1-32 amphipathic α-helix of SCP-2 functionally interacted with caveolin-1. This interaction was independent of the classic caveolin-1 scaffolding domain in which many signaling proteins interact. Instead, SCP-2 bound caveolin-1 through a new domain identified in the N-terminal domain of caveolin-1 between amino acids 32-55. Modeling studies suggested that electrostatic interactions between the SCP-2 N-terminal aa1-32 amphipathic α-helical domain (cationic, positively charged face) and the caveolin-1 N-terminal aa33-59 α-helix (anionic, negatively charged face) may significantly contribute to this interaction. These findings provide new insights on how SCP-2 enhances cholesterol retention within the cell as well as regulates the distribution of signaling lipids such as phosphoinositides and sphingolipids at plasma membrane caveolae.

Keywords

sterol carrier protein-2; caveolae; caveolin-1; caveolae; cholesterol; signaling

Increasing evidence indicates that cholesterol found at the cell surface plasma membrane (PM) is not randomly distributed, but instead organized into both transbilayer (1,2) and lateral (3,4) cholesterol-rich (and/or sphingolipid-rich) domains that adopt a unique, liquid-ordered structural organization (4–7). It has been postulated that this self-assembling property of cholesterol (and also sphingolipids) into domains in turn forms the structural basis for selective membrane protein organization (8). Support for this hypothesis is from numerous studies demonstrating that many PM proteins are functionally organized into lipid rafts and/or caveolae, a sub-fraction of lipid rafts that have proven to be a remarkably stable

†**Acknowledgments:** This work was supported in part by the USPHS National Institutes of Health GM31651 (FS and AK) and GM62326 (JMB).

[*]**Corresponding author at:** Department of Pathobiology, Texas A&M University, TVMC, College Station, TX 77843-4467, Phone: (979)845-7910, FAX: (979)845-9231, Jball@cvm.tamu.edu.
[‖]**Current Address:** Department of Internal Medicine, University of Texas Southwest Medical Center, Dallas, TX 75390

structural and functional entity (9,10). Diverse processes such as transmembrane signal transduction (e.g. eNOS, estrogen, insulin), the action of microbial (e.g. cholera toxin) and viral (e.g. NSP4) toxins, potocytosis, and microbial (viruses, bacteria, protozoa) entry into cells are mediated through PM lipid rafts/caveolae (rev. in (4,11,12). Depletion of cholesterol from the PM lipid rafts/caveolae disrupts these functions. Due to these findings, it has become increasingly important to resolve how cholesterol is transported to lipid rafts/caveolae and how the distribution of cholesterol is regulated within these domains.

Because of the importance of cholesterol to membrane domains and other cell functions, it is not surprising that mammalian cells have evolved multiple pathways for cholesterol entry/efflux. First, unidirectional uptake of cholesteryl ester and cholesterol is mediated by the classic low density lipoprotein (LDL) receptor/lysosomal endocytic pathway (13). Second, unidirectional 'selective cholesterol uptake' is mediated by high density lipoprotein (HDL) binding to scavenger receptor B1 (SRB1) at PM. SRB1 lacks a consensus caveolin 'scaffold binding domain' (14), and is localized not only in caveolae (e.g. fibroblasts, endothelial cells) but also in lipid rafts of caveolin-1 deficient cells (e.g. hepatocytes) (14–17). Once bound to SRB1, HDL cholesteryl ester is transferred to the PM lipid rafts/caveolae, internalized by an unresolved, non-endocytic process and undergoes hydrolysis by non-lysosomal, neutral esterases to free cholesterol (17,18). Third, unidirectional cholesterol efflux occurs via the ATP-binding cassette transporter A1 (ABCA1) (19–21) which localizes to lipid rafts/caveolae (22,23). ABCA1 binds apoprotein-1 (apoA1) to enhance phospholipid efflux, followed by ABCA1 independent cholesterol transfer to the phospholipid containing apoA1, which then becomes HDL (21,24) . Fourth, the bidirectional cholesterol uptake/efflux pathway in which HDL binds to SRB1 is localized in lipid rafts/caveolae rafts and donates/takes up cholesterol by a process that is as yet unclear (15,16,21). Although caveolin-1 expression is associated with increased cholesterol transport to caveolae and increased cholesterol efflux to HDL (14,17,25), SRB1 localization in caveolae is not required for cholesterol uptake/efflux15. While there is considerable evidence that the multi-drug resistance transporter P-glycoprotein (P gp) also participates in SRB1-mediated cholesterol transfer to/from bound HDL, it remains unclear whether P-gp resides in caveolae (26), in non-caveolar lipid rafts (27), or in an intermediate density membrane microdomain distinct from caveolae and classical lipid rafts 28. Many of these proteins appear to indirectly regulate/alter cholesterol flux between the PM and HDL by acting as phospholipid flippases (e.g. ABCA1, P-gp) (21,24,28,29). Photocrosslinking and immunoprecipitation studies show that: (i) caveolin-1 (30,31), but not ABCA1 (24) or SRB1 (14), directly binds cholesterol; (ii) ABCA1 and SRB1, but not caveolin-1, directly bind HDL (21,22); (iii) While neither ABCA1, P-gp, or SRB1 contain a caveolin-1 'scaffold binding domain', ABCA1 may interact directly with caveolin-1 (22). Thus, by directly binding caveolin-1 the ABCA1 may provide a scaffolding platform for cholesterol efflux through either the SRB1 or ABCA1 pathways.

Both vesicular and protein mediated pathways appear to contribute to intracellular trafficking of cholesterol to and from lipid rafts/caveolae (4,17,32–34). At least three cholesterol binding proteins may be involved in protein-mediated cholesterol trafficking through the cytoplasm: caveolin-1, sterol carrier protein-2 (SCP-2), and liver fatty acid binding protein (L-FABP) (4,35,36). Bidirectional flux of free cholesterol and unidirectional uptake of cholesterol ester is thought to be mediated by cytoplasmic transport complexes of caveolin-1, cholesterol (or cholesterol ester), and one or more chaperone proteins (cyclophilin A, cyclophilin 40, heat shock protein 56, and/or annexin II). The mechanism(s) whereby these complexes dock/interact with PM caveolae appears to involve the CD44 receptor and cytoskeletal proteins (17). In contrast to caveolin-1, the other cholesterol binding proteins (L-FABP, SCP-2) have been reported to form simple molecular complexes with cholesterol (but not cholesteryl ester) to (i) enhance cholesterol uptake (SCP-2 >> L-

FABP), (ii) transfer cholesterol between membranes with which they interact (SCP-2>>L-FABP), and (iii) transfer of cholesterol into bile (L-FABP) (35,37–43). Notably, SCP-2 expression not only enhances cholesterol uptake (44) and stimulates intracellular cholesterol esterification (45,46) while concomitantly inhibiting cholesterol efflux to HDL (33). These findings suggest that caveolin-1 and SCP-2 may have antagonistic effects depending on the cell context. As yet, relatively little is known about the mechanism(s) whereby caveolin-1/cholesterol/chaperone, L-FABP cholesterol, and SCP-2 cholesterol complexes dock/interact with PM lipid rafts/caveolae.

Caveolin-1-interacting proteins have been shown to bind the caveolin-1 scaffolding domain (CSD) that resides in amino acids (aa) 80-101 of the central region of caveolin-1 (47). The caveolin-1 binding domain (CBD) is comprised of the recognition sequence ΦXΦXXXXΦor ΦXXXXΦXXΦ, where Φ is an aromatic residue (Trp, Phe, or Tyr) (12,48,49). Recent data from our laboratory show SCP-2 is in close proximity to caveolin-1 (i.e. 48±4 Å, as determined by fluorescence resonance energy transfer (FRET) and immunogold electron microscopy), suggesting a direct interaction with caveolin-1 (50). Yeast two-hybrid and co-immunoprecipitation assays confirm these findings (50). However, examination of the SCP-2 aa sequence reveals that this protein lacks a consensus caveolin-1 binding domain (50) . The purpose of the present investigation was to use a series of caveolin-1 mutants and yeast two-hybrid assays to determine: (i) if SCP-2 interacts with caveolin-1 through the scaffolding domain, and if not, (ii) whether SCP-2 interacts with another caveolin-1 domain. These studies contribute significantly to our understanding of how SCP-2 participates in intracellular cholesterol trafficking and/or cholesterol uptake/efflux through caveolae.

MATERIALS AND METHODS

Materials

CNBr-activated sepharose 4B beads were obtained from Amersham Biosciences (Piscataway, NJ). SCP-2 and caveolin-1 peptide-specific antibodies were generated in rabbits in our laboratory as described (50–53). Rabbit anti-human caveolin-1 was purchased from Jackson Immunoresearch Labs Inc. (West Grove, CA) or Transduction Labs (San Diego, CA). Bound antibodies were detected by horseradish peroxidase (HRPO) labeled goat anti-rabbit IgG (Kirkegaard & Perry Laboratories, Inc, Gaithersburg, MD or Pierce, Rockford, IL). Total protein was quantitated using the BCA protein assay kit (Pierce). Dulbecco modified Eagle medium (DMEM) was from Gibco (Grand Island, NY). Fetal bovine serum (FBS), glutamine, penicillin-streptomycin (100 μg/ml) and non-essential amino acid (1X) were from Sigma (St. Louis, MO).

Mammalian cell culture

MDCK cells were obtained from ATCC (Rockville, MD) and maintained in DMEM supplemented with 10% FBS, glutamine (2 mM), penicillin-streptomycin (100 μg/ml) and non-essential amino acid (1X). Due to the high expression level of caveolin-1 in MDCK cells (53), MDCK lysates were prepared as a source of caveolin-1 antigen. Murine L-cells (L arpt-tk-) were cultured as previously described (54).

Yeast strains for two-hybrid assay

Saccharomyces cerevisiae strain MaV203 (MATα, Ieu2-3,112, trp1-901, his3Δ200, ade2-101, gal4Δ, gal80Δ, SPAL10::*URA3*, GAL1::lacZ, $HIS3_{\text{uas gal1}}$::*HIS3*@LYS2, can1^{r}, cyh2^{r}) was used for all two-hybrid analyses (55). A collection of yeast strains that contain plasmid pairs expressing fusion proteins with a spectrum of interaction strengths [pPC97 (GAL4-DB, LEU2), pPC97-CYH2^{s} and pPC86 (GAL4-AD, TRP1)] were used as

controls(53,56–59). The control plasmids pDBIeu and pEXP-AD507 contain only the Gal4 DNA-binding domain (BD) and the Gal4 activating-domain (AD) respectively.

The *S. cerevisiae* yeast strain InVSc1 (MATα his3-Δ1, Ieu2, trp1-289, ura3-52; Invitrogen) was used to induce the production of full length caveolin-1, mutant caveolin-1 and SCP-2 proteins.

Construction of plasmids

SCP-2 and full length caveolin-1 cDNA were cloned into the Invitrogen Gateway™ Destination vectors pDEST22 and pDEST32 (ProQuewst Two hybrid system with Gateway Technology Manual, Invitrogen Life Technologies Inc.) as previously described (53,55). The deletion mutant clones of caveolin-1, Caveolin-1-156, 60-178, Δ60-100 and Δ83-123, were constructed by site-directed mutagenesis using the primers described to the right of the schematic representation of the deletion mutants (Fig. 1).

All plasmid manipulations were performed according to standard protocols in the Escherichia coli strains DH5α (ProQuewst Two hybrid system with Gateway Technology Manual, Invitrogen Life Technologies Inc.). The PCR products were directionally cloned into the Gateway™ System entry vector, pENTR11 (Invitrogen, CA), sequence verified, subcloned into the destination vectors of the Gateway™ Expression System, pDEST 22 (Gal4 activation domain [AD]-X) and pDEST32 (Gal4 DNA binding domain [BD]-Y). Briefly, 300 ng of the pENTR11-SCP-2/caveolin-1 plasmids were incubated with 300 ng of the destination vector, pDEST22 or pDEST32, LR Buffer, TE (1X), and the LR Clonase Enzyme Mix (Invitrogen). The resultant clones were transformed into DH5α and plated onto LB plates with 100 μg/ml ampicillin or 7 μg/ml gentamycin. Following amplification, recombinant plasmids were extracted using the Wizard Miniprep Kit (Promega), restriction enzyme digested with EcoRV, Kpnl, or Xhol (Promega), and sequence verified. Fusion protein expression levels were monitored by Western blot analyses.

Expression of SCP-2, caveolin-1 and mutant caveolin-1 in yeast

The entry level clones (pENTR11) used to create the yeast two-hybrid expression clones were also employed to introduce the sequences encoding SCP-2, caveolin-1 and mutant caveolin-1 proteins into the inducible yeast expression plasmid, pY52DEST (Invitrogen) as described above. Transformants were first grown on CSMUra$^-$ plates, transferred to liquid CSMUra$^-$, and induced with galactose in YPAG [yeast extract, peptone, and 2% galactose (Difco)] medium to express full length SCP-2 and caveolin-1, or the four deletion caveolin-1 mutants. Briefly, cells were grown in liquid CSMUra$^-$ medium at 30°C for 24 h, washed and resuspended at an OD_{600} of 0.5 in YPAG and incubated at 30°C for 24 h. Yeast protein cell lysates were prepared using the Zymo Yeast Protein Extraction kit (Zymo Research, Orange, CA) as previously described (50) and used in the binding and Western blot assays to detect SCP-2, caveolin-1 or mutant caveolin-1 proteins. Briefly, approximately 1×10^6 cells were pelleted, Y-lysis buffer and zymolase were added, and the samples incubated at 37°C for 1h. The cells were centrifuged at 400g for 5 min, and supernatants were removed. The pellets were resuspended into PBS with protease inhibitors (100μM AEBSF, 80nM Aprotinin, 5μM Bestatin, 1.5μM E-64, 2μM Leupeptin, 1μM Pepstatin A, 100μM PMSF, Calbiochem-Novabiochem Corp., San Diego, CA). Total protein in each pellet was quantitated using the BCA protein assay kit (Pierce). Approximately 10 μg of each pellet was separated on a 12% SDS-PAGE, transferred to nitrocellulose and probed with rabbit polyclonal SCP-2 or caveolin-1 antibodies (50,53). The primary antibodies were detected using goat anti-rabbit-HRP antibodies (Pierce) followed by addition of the Super Signal Pico West Chemiluminescent Substrate (Pierce), and bands were visualized using X-OMAT film (Kodak).

Yeast Two-Hybrid Screening

S. cerevisiae strain MaV203 (MATα, Ieu2-3,112, trp1-901, his3Δ200, ade2-101, gal4Δ, gal80Δ, SPAL10::*URA3*, GAL1::lacZ, $HIS3_{uas\ gal1}$::*HIS3*@LYS2, $can1^r$, $cyh2^r$) was used to test for protein:protein interactions of SCP-2 and either caveolin-1 or the mutants of caveolin-1 (58,59). A panel of MaV103 (MATα) control strains containing the same genotype as MaV203 expressing a GAL4 DNA binding fusion protein (DB-X) and a GAL4 transcription activating protein (AD-Y) fusion proteins with a spectrum of interaction strengths were replica plated onto assay plates (49–52). The control vectors were pPC97 (GAL4-DB, LEU2), pPC97-$CYH2^S$ and pPC86 (GAL4-AD, TRP1). pDBIeu and pEXP-AD507 contain only the Gal4 DNA-binding domain (BD) and the Gal4 activating-domain (AD) respectively. All plasmid manipulations were performed according to standard protocols for the *E. coli* strains DH5α (48,53,54). MaV203 yeast were transformed by a modified lithium acetate (LiAc) procedure as previously described (56–59). Briefly, *S. cerevisiae* MaV203 were grown in YPAD overnight at 30°C, diluted to an OD_{600} of 0.5, and incubated at 30°C with shaking to an OD_{600} of 2. The cells were pelleted, washed with distilled H_2O, resuspended in 1 ml of 100mM LiAc, pelleted, and resuspended in 0.4 ml of 100mM LiAc, and 50 μL aliquots were pelleted. The following solutions were added in order: 240 μL of 50% PEG (3350 M_r); 36 μL of 1M LiAc, 25 μL of salmon sperm DNA (2mg/ml); 50 μL of $_dH_2O$; and 100 ng of each plasmid DNA.

Transformants were grown at 30°C for 3 days on complete synthetic medium lacking leucine and tryptophan ($CSMLeu^-Trp^-$) to identify colonies containing both plasmids. To determine the two-hybrid-dependent transcription activation by SCP-2 and caveolin-1 or mutants of caveolin-1, the induction of the reporter genes, *URA3* and *HIS3*, was evaluated by monitoring the yeast growth patterns on $CSMLeu^-Trp^-Ura^-$, $CSMLeu^-Trp^-$ + 0.2% 5FOA, $CSMLeu^-Trp^-His^-$ + 3AT (12.5mM, 50mM and 100mM 3AT) (50,53). Activation of the *LacZ* promoter was detected qualitatively using the substrate X-gal (5-bromo-4-chloro-3-indolyl-β-D-galactopyranoside). To quantitatively measure β-galactosidase activity, chlorophenol red-β-D-galactopyranoside (CPRG) was used as substrate (50). To ensure that the DB-X or the AD-Y fusion proteins do not function as transcription activators, yeast were transformed with the individual fusion constructs and evaluated for growth on all the media described above.

Western Blot Assays

The colonies that appeared positive for protein-protein interactions as determined by the phenotypic growth patterns were grown in liquid $CSMLeu^-Trp^-$ and yeast protein extracts were prepared using the Zymo Yeast Protein Extraction kit (Zymo Research, CA). In brief, cells were grown in YPAD medium overnight at 30°C, 1×10^6 cells were pelleted, lysed with zymolase, resuspended in PBS, pH 7.2, containing protease inhibitors (above), and quantified by BCA (Pierce). All lysates were separated by 12% SDS-PAGE, electroblotted onto nitrocellulose membranes, probed with SCP-2 or caveolin-1 peptide-specific antibodies and horseradish peroxide (HRP)-conjugated antibodies as previously described (50,53,55).

Protein purification

The human recombinant mature 13 kDa SCP-2 and 15 kDa pro-SCP-2 were purified as described earlier (60). PEX 5C was generously provided by Dr. Jeremy Berg (Johns Hopkins University).

In vitro caveolin-1 SCP-2 binding assay

To confirm the interactions of caveolin-1 and 13 kDa SCP-2 determined by the yeast two-hybrid assay, an *in vitro* binding assay was developed. Synthetic peptides corresponding to

caveolin-1 residues 2–31, 19–40, 34–55, 76–101, and 161–178 (Table 1), a peptide corresponding to mature 13 kDa SCP-2 aa 1-32 (SCP-2_{1-32}), a peptide wherein residue aa20L was mutated to E (SCP-$2_{1-32E20}$), and a peptide corresponding to the 20 aa presequence of pro-SCP-2 (pro-SCP-2_{1-20}) present in 15 kDa pro-SCP-2 (61,62) were synthesized as described earlier (Table 1) (63–65). SCP-2 residues 1–32 contain the N-terminal amphipathic α-helical region of mature 13 kDa SCP-2 and represent the membrane interaction domain of SCP-2 (63–65).

The peptides described above were attached to CNBr-activated sepharose 4B beads as recommended by the manufacturer (Amersham Biosciences Corp., Piscataway, NJ). Aliquots (2 mg total protein each) of lnVSc-1 (does not express caveolin-1) or MDCK lysate (expresses caveolin-1) were incubated with 50 μI of a 50% slurry sepharose 4B or sepharose 4B-SCP-2_{1-32} overnight at 4°C with gentle mixing. The beads were pelleted by centrifugation, washed 3 times with wash buffer (10 mM Tris pH 7.5, 0.5 M NaCI) and resuspended in PBS containing protease inhibitors (above). Half of each sample was separated by 12% SDS-PAGE, transferred to nitrocellulose membranes and probed with rabbit anti-caveolin-1 in Western blot assays as described above. Interaction(s) of caveolin-1 mutants with SCP-2_{1-32} also were monitored with full-length caveolin-1, Caveolin-1-156, and Caveolin-160-178 that were expressed in InVSc1 yeast.

To verify the specificity of the reactivity of purified SCP-2 with Cav_{19-40}- and Cav_{34-55}-bound sepharose beads (Fig. 5B), the integrated density value (IDV) for each band was determined using a Fluorochem™ 8000 Advanced Imager (Alpha Innotech Corp.). The average value after background correction was plotted at different concentrations of purified SCP-2 and a constant peptide concentration.

Role of pro-SCP-2 N-terminal presequence for targeting to peroxisomes: *in vitro* Fluorescence Resonance Energy Transfer (FRET)

To determine the relative affinity of the C-terminal peroxisomal targeting sequence-1 (PTS-1) present in both SCP-2 and pro-SCP-2, the interaction of these proteins with PEX 5C (peroxisomal receptor for the PTS-1) was examined by FRET. Recombinant PEX 5C was covalently labeled with Cy3 (fluorescence donor) while SCP-2 or pro-SCP-2 were labeled with Cy5 (fluorescence acceptor) by use of a Fluorolink-antibody Cy3 and Cy5 labeling kit (Amersham Biosciences) as indicated by the manufacturer's instructions. A fixed amount of donor (10nM PEX 5C) was incubated with increasing amounts of acceptor (Cy5-SCP-2 or Cy5-pro-SCP-2) in phosphate buffered saline, pH 7.4, 24°C. Cy3-was excited at 550nm and emission was scanned from 560-700nm using a PC1 photon counting spectrofluorometer (ISS Inc., Champaign, IL), and the data was corrected for background (buffer only, donor only, and acceptor only). Binding affinities were calculated from quenching of Cy3 fluorescence intensity (Fo-F) at 570nm with increasing acceptor concentration as described earlier (66). The intermolecular distance was calculated as shown previously using the known critical distance for 50% efficiency (i.e. 50Å:) for the Cy3/Cy5 FRET pair (67).

Laser Scanning Confocal Microscopy (LSCM) of SCP-2 Colocalization with Caveolae/Lipid Raft Marker GM_1 at the Plasma Membrane of Living Cells

Murine L-cells (Larpt-tk-) were seeded onto Lab-Tek chambered cover glass slides as previously described (54). Culture medium was replaced with 0.5ml of serum-free media containing 0.7 g of protein (Cy5-labeled SCP-2 or Cy5-labeled pro-SCP-2 prepared as described above) per chamber well and incubated at 37°C and 5% CO_2 in a humidified chamber for 1 hour. Thereafter, 1ml of complete media (containing serum) was added to each chamber well and cells were incubated for an additional 2 hours as described above. Cells were washed with 1 ml cold PBS four times and after the final wash incubated at 4°C

for 10 min. PBS wash was replaced with cold PBS containing 0.4 g/ml cholera toxin B-AF488 (Invitrogen Corp.) and cells were incubated at 4°C for an additional 5 min before imaging. Cholera toxin B is a select marker for ganglioside M_1 (GM_1) in caveolae/lipid rafts (7,51). LSCM was performed with a MRC-1024 fluorescence imaging system (Bio-Rad, Hercules, CA) equipped with a Axiovert 135 microscope and X63 Plan-Fluor oil immersion objective, N.A.1.45 (Zeiss, Carl Zeiss Inc., Thornwood, NY). AlexaFluor 488 and Cy5 probes were excited at 488/647 lines with a krypton-argon laser (5mW, all lines) (Coherent, Sunnyvale, CA) set at 10% scan strength, and emission was simultaneously recorded by separate photomultipliers after passing through a 540/30 or 680/32 emission filter, respectively under manual gain and black level control.

RESULTS

SCP-2 interacts with caveolin-1 in a yeast two-hybrid assay

Although SCP-2 lacks a CBD consensus sequence for interacting with the CSD, the possibility was considered that SCP-2 may still interact through some other interaction with this domain or with another region of caveolin-1. The sequences encoding SCP-2, full-length caveolin-1 (Caveolin-1 1-178), and caveolin-1 deletion mutants (Fig. 1) were cloned into the ProQuest (Invitrogen) vectors pDEST32 and pDEST22 to produce fusion proteins encoding the GAL4 DNA -binding domain and -activating domain, respectively. The resultant plasmids were co-transformed into yeast (MaV203), and initially grown on $CSMLeu^{-}Trp^{-}$ plates with transformation efficiencies of ~ 2–5 × 10^6 transformants/μg plasmid DNA (data not shown). These data are in the range of the standard efficiencies of greater than 1 × 10^6 transformants/μg plasmid DNA (49).

Co-transformed yeast were monitored for growth on media lacking specific aa and incorporating specific growth inhibitors. Four phenotypes, $His^{+}(3AT^{R})$, β-gal, Ura^{+} and $5FOA^{S}$ were used to assess the activation of the chromosomally integrated reporter genes, *HIS3, URA3*, and *LacZ*. Both the control yeast that are supplied with the ProQuest™ Two-Hybrid System, and the transformants grew on plates with $CSMLeu^{-}Trp^{-}$, demonstrating the presence of both co-transformed plasmids, pDest32 and pDest22 vectors (Table II). Induction of the *URA3* gene was shown with growth on $CSMLeu^{-}Trp^{-}Ura^{-}$ plates and the inhibition of growth on $CSMLeu^{-}Trp^{-}$ + 0.2% 5FOA. The *URA3* promoter, SPO13, previously has been shown to be a weak promoter, yielding low growth of yeast on plates lacking uracil. The data presented in Table II were consistent with this finding. Induction of *HIS3* was demonstrated by showing an increased 3AT dose-dependent level of inhibition of growth on $CSMLeu^{-}Trp^{-}His^{-}$ + 3AT in agreement with the *URA3* data (Table II). The induction of *LacZ* resulted in positive yeast colonies turning a blue color when assayed on nitrocellulose membranes using X-gal as the substrate (data not shown). All colonies that demonstrated phenotypes interpreted by the four reporter gene readouts as ‘possible interactors’ with weak to little production of β-galactosidase and/or uracil, were confirmed and quantitated using the liquid CPRG assay for *LacZ* expression (Table II). Taken together, the growth patterns of the co-transformed yeast confirmed the activation of the three reporter genes in the yeast two-hybrid assays and established SCP-2 and caveolin-1 as forming a true protein:protein interaction.

Localization of the binding site of SCP-2 to the N-terminal region of caveolin-1

The following deletion mutants were utilized to determine the region of caveolin-1 that interacts with SCP-2: (i) Caveolin-1 1-156, a C-terminal deletion mutant of Cav-1 missing most of C-terminal cytoplasmic domain, (ii) Cav 60-178, a N-terminal deletion mutant of caveolin-1 missing almost all of the N-terminal cytoplasmic domain except for the signature domain, (iii) Cav Δ83-123, a caveolin-1 deletion mutant missing part of the caveolin-1

scaffolding domain and part of the transmembrane domain, and (iv) Cav Δ60-100, a caveolin-1 deletion mutant missing all of the scaffolding domain and signature domain. Yeast co-transformed with pD22-caveolin-1, -Caveolin-1 1-156, - Cav Δ83-123, - Cav Δ60-100and pD32-SCP-2 demonstrated the correct phenotypes (interaction with SCP-2) on the selection media and β-galactosidase activity equal to or greater than the 1+ positive control (data not shown). Likewise, when caveolin-1 and mutants were cloned into pD32 and co-transformed with pD22-SCP-2, the correct phenotypes (interaction with SCP-2) on the selection media were observed, and β-galactosidase activity was equal to or greater than the 1 + positive control (Table II). However, yeast co-transformed with the fusion construct, pD32Cav 60-178 and pD22SCP-2 failed to demonstrate the correct phenotypes on the test media for a protein-protein interaction and were negative for β-galactosidase activity in both the X-gal assay (data not shown) and CPRG assay (Table II). These results strongly suggest that caveolin-1 does not bind SCP-2 through the scaffolding domain, the C-terminal cytoplasmic tail, or the signature domain. Instead, the binding site of caveolin-1 for SCP-2 was localized to the N-terminal cytoplasmic domain comprised of caveolin-1 residues 1–59.

SCP-2 and caveolin-1-GAL4 DNA-binding domain- and activating domain-fusion proteins were present in the co-transformed yeast

Expression of both fusion proteins in co-transfected yeast was confirmed by western blot analyses (Fig. 2). The GAL-4 fusion proteins were observed when the yeast lysates were electroblotted and probed with either SCP-2-specific peptide antibodies or caveolin-1 antibodies (Fig. 2). In figure 2A, the co-transformed yeast lysates containing pD32-caveolin-1 full length or mutants and pD22-SCP-2 showed a SCP-2 fusion protein at the same Mr (~25.5 kD, lanes 2–5). Whereas in figure 2B, the caveolin-1 fusion proteins were seen as a dimer (Mr between 60-78 kD). For example, pD32-cav Δ83-123 should run at ~62.8 kD as Gal4 calculates as ~16.8 kD and cav Δ83-123 as ~14.6 kD making the monomer ~31.4 kD and the dimer ~62.8 kD (lane 2) and pD32-caveolin-1 calculates to ~38.8 kD monomer and ~77.6 kD dimer (lane 5). These data corroborated that the fusion proteins encoded on both plasmids were translated in the yeast.

Direct interaction of caveolin-1 with SCP-2 *in vitro*: Role of the SCP-2 N-terminus

The caveolin-1 scaffolding domain (aa 80-100) represents not only the binding sites for numerous proteins (48,49), but also the membrane lipid raft binding site (68,69). By analogy, although the SCP-2 N-terminal aa 1-32, an amphipathic α-helix structure (i.e. hydrophobic face and cationic face), comprises an SCP-2 structural domain for interaction with model membranes containing anionic phospholipids (63–65), it is not known whether SCP-2_{1-32} comprises a protein binding (e.g. caveolin-1) domain. To begin to resolve this issue, the N-terminal SCP-2_{1-32} was synthesized, coupled to sepharose 4B beads, and used in an *in vitro* binding assay wherein caveolin-1 binding was detected by Western blot analyses. Synthetic peptides corresponding to caveolin-1 residues 2–31, 19–40, 34–55, 76–101, and 161–178 (Table 1), a peptide corresponding to mature 13 kDa SCP-2 aa 1-32 (SCP-2_{1-32}), a peptide wherein residue aa20L was mutated to E (SCP-$2_{1-32E20}$), and a peptide corresponding to the 20 aa presequence of pro-SCP-2 (pro-SCP-2_{1-20}) present in 15 kDa pro-SCP-2 (61,62) were synthesized as described earlier (Table 1) (63–65)To confirm the *in vivo* yeast two-hybrid assay that identified the caveolin-1 N-domain as the interaction site with SCP-2, the *in vitro* peptide binding assay was repeated using yeast lysates expressing full length caveolin-1 (pY52DCaveolin-1), a caveolin-1 mutant with the putative binding site present (e.g. pY52DCaveolin-1 1-156), and an N-terminal deletion mutant of caveolin-1 with the putative binding site deleted (e.g. pY52DCav 60-178) (Fig. 3B). The lack of reactive bands in lanes 1, 2, 3, and 7 (Fig. 3B) showed the lack of non-specific binding of the sepharose-4B beads and specificity of the antibody. SCP-2_{1-32}-linked beads bound to full length α-caveolin-1, but not β-caveolin-1 (Fig. 3B, lane 4). In contrast,

SCP-2_{1-32}–linked beads bound to both α- and β-caveolin-1 1-156 missing the C-terminus (Fig. 3B, lane 5). Cav 60-178 failed to bind the SCP-2_{1-32}-linked beads (lane 6). Taken together, these findings not only confirm that the SCP-2_{1-32} binding site is localized to the N-terminus of α-caveolin-1, but that interaction with the shorter β-caveolin-1 (missing the N-terminal 32 aa present only in α-caveolin-1) became more prominent upon deletion of the caveolin-1 C-terminus. These data suggest that the N-terminal SCP-2 interacted with the N-terminus of full length α-caveolin-1, but interacted with β-caveolin-1 only when the α-caveolin-1 C-terminus was missing.

Because SCP-2_{1-32} bound the N-terminus of caveolin-1, it was important to determine if this correlated with the ability of this SCP-2 domain to bind anionic phospholipids. SCP-2_{1-32} contains an amphipathic helical region containing a basic face, which directly interacts with anionic phospholipids in model membranes (63,64). Therefore, the amphipathic helical region of SCP-2_{1-32} was disrupted by replacing Leu20 with Glu20 to produce the mutant peptide SCP-$2_{1-32E20}$ In this study, SCP-$2_{1-32E20}$ was coupled to beads and binding to caveolin-1 was determined with the *in vitro* peptide binding assay using yeast lysates expressing full-length caveolin-1 and caveolin-1 deletion mutants. SCP-$2_{1-32E20}$ interacted with full length α-caveolin-1 (Fig. 3C, lane 3) and with caveolin-1 deletion mutants, Caveolin-1 1-156 (Fig. 3C, lane 4), but not with the Cav 60-178 (Fig. 3, lane 5). Again Western blotting also showed that SCP-$2_{1-32E20}$ primarily interacted only with the full length α-caveolin-1 form (Fig. 3C, lane 4), but also interacted with the β-caveolin-1 when the C-terminus was deleted (Fig. 3C, lane 4). Note that SCP-$2_{1-32E20}$ does not bind to anionic phospholipids (63,64) and does not exhibit lipid transfer activity (70). Thus, the ability of SCP-2_{1-32} to interact with the N-terminal region of caveolin-1 shown herein is independent of its ability to bind to anionic phospholipids (63,64) and elicit lipid transfer (70).

To determine if the 20 aa amino acid pre-sequence present in pro-SCP-2 also interacted with caveolin-1, pro-SCP-2_{1-20} was linked to beads and tested for binding to full-length and mutant caveolin-1, pro-SCP-2_{1-20}-linked beads predominantly bound to full length α-caveolin-1 (Fig. 3D, lane 4), whereas pro-SCP-2_{1-20} bound to both α- and β-caveolin-1 when the caveolin-1 C-terminus was deleted (Fig. 3D, lane 5), but not to Cav 60-178 (Fig. 3D, lane 6). Lane 8 of Fig. 3D shows that the yeast express both isoforms of caveolin-1. Thus, in the mature SCP-2, the caveolin-1 binding site was localized in SCP-2_{1-32}, while in the pro-SCP-2 precursor the 20 aa N-terminal presequence also bound. Taken together these data indicate the SCP-2 caveolin-1 binding site is localized to the N-terminus, as suggested with the yeast two-hybrid data, and the caveolin-1 binding also occurs with the 20 aa presequence present of pro-SCP-2.

To examine the caveolin-1-SCP-2 interaction in greater detail, synthetic peptides corresponding to caveolin-1 residues 2–31, 19–40, 34–55, 76–101, and 161–178 were synthesized and attached to CNBr-activated sepharose 4B beads. In addition, SCP-2 was purified to test the reactivity to the different caveolin-1 peptides in a direct binding assay. The silver stain (inset) and mass chromatogram show the purity of the SCP-2 protein (Fig. 4).

Purified SCP-2 and recombinant yeast lysates expressing SCP-2 were reacted with the panel of caveolin-1 synthetic peptides bound to sepharose beads (Fig. 5). Note in all assays the beads alone (no peptide) incubated with InVSc1 lysates were non-reactive. In figure 5A, Cav_{2-31}-bound beads also failed to react with InVSc1 or pY52D-SCP-2 (lanes 2 and 5, respectively). Similarly, Cav 76-101 and 161-178 failed to bind purified SCP-2 (data not shown) or SCP-2 expressed in yeast (Fig. 5C and 5D). When the caveolin-1 N-terminal peptides, $Cav1_{19-40}$ and $Cav1_{34-55}$, were reacted with purified SCP-2, a strong interaction

was noted (Fig. 5B, lanes 2 and 3). However, there was a minor interaction between the beads alone with purified SCP-2 (Fig. 5B, lane 1). This pattern was repeatedly observed with purified SCP-2 varying in concentration from 50–200 ng and a constant concentration of bound-peptide or beads alone. To rectify this background reactivity, the integrated density value (IDV) of equal areas was established for each concentration of SCP-2 reacted against the N-terminal caveolin-1 peptides. The IDV of the light band corresponding to beads alone and SCP-2 were subtracted from the positive values and plotted (Fig 5E). As shown with both 200 ng and 50 ng of purified SCP-2, the IDV of SCP-2 and Cav_{19-40} was consistently higher than that observed with Cav_{34-55} suggesting SCP-2 had higher affinity for Cav_{19-40} than for Cav_{34-55} (Fig. 5E). Taken together, these data indicate a specific interaction between SCP-2, and Cav_{19-40} and Cav_{34-55}, with a stronger binding with Cav_{19-40}.

In summary, the results of the *in vivo* yeast two-hybrid assays indicated that the caveolin-1 cytoplasmic N-terminal 59 aa contained the SCP-2 binding domain. The *in vitro* binding assays using $SCP\text{-}2_{1-32}$ confirmed the N-terminus of SCP-2 binds to an N-terminal region of caveolin-1 and refined the SCP-2 binding site to the first 32 residues (Fig. 7). Subsequent caveolin-1 peptide binding assays using purified or recombinant SCP-2 localized the binding domain of SCP-2 to caveolin-1 to $Cav1_{19-40}$ and $Cav1_{34-55}$ or caveolin-1 residues 19-55, which can be further defined to amino acids 32-55 when considering the negative binding results of SCP-2 to $Cav1_{2-31}$. (Fig. 5&Fig. 7). These data further indicated a stronger reactivity between SCP-2 and the 19-40 caveolin-1 peptide when compared to the 34-55 peptide.

Role of the N-terminal pre-sequence of pro-SCP-2 in receptor interactions *in vitro*

As indicated above, the 20 aa presequence of pro-SCP-2 also interacted with caveolin-1, albeit the functional significance of this finding is not known. Western blot analyses detect only the mature SCP-2, suggesting that the pro-SCP-2 interaction is not physiologically significant (rev in (39). However, convincing evidence has been presented that demonstrates the pro-SCP-2 is significantly more targeted to peroxisomes where the 20 aa presequence is proteolytically cleaved (rev. in (39). This suggests that the 20 aa presequence might be more important for interaction of the pro-SCP-2 with the peroxisomal receptor (PEX 5C), in which the peroxisomal targeting sequence-1 is present in the C-terminus of pro-SCP-2 as well as SCP-2. To examine the latter possibility, a FRET assay was used to determine binding affinities of PEX5C for pro-SCP-2 vs SCP-2 as described in Methods. PEX5C bound pro-SCP-2 with high affinity, K_d of 2.3 nM, over 12-fold stronger than that for SCP-2 (Table 3). Consistent with the close molecular interaction between PEX5C and these proteins, the respective intermolecular distances were both near 70 Å (Table 3). Further, the intermolecular distance between pro-SCP-2 and PEX5C in the complex was slightly larger than between SCP-2 and PEX5C, reflecting the larger size of the 15 kDa pro-SCP-2 as compared to 13 kDa SCP-2, (Table 3). These data indicate the pro-SCP-2 interacts significantly more strongly with the peroxisomal receptor PEX5C than does SCP-2 ($p<0.05$).

Role of the N-terminal pre-sequence of pro-SCP-2 in determining SCP-2 distribution to plasma membrane lipid rafts in living cells

To determine if the presence of the N-terminal presequence in pro-SCP-2 resulted in less targeting to plasma membrane caveolae/lipid rafts, SCP-2 was colocalized with GM_1 (caveolae/lipid raft marker) by laser scanning confocal microscopy (LSCM). When L-cells were incubated with the same amounts of Cy5-SCP-2 or Cy5-pro-SCP-2 as described in Methods, these proteins were taken up by the cells to similar extent (not shown). However, labeling of the intact cells with cholera toxin B-AF488 (marker for GM_1) revealed significant differences in colocalization at plasma membrane caveolae. When Cy5 and

cholera toxin B-AF488 were simultaneously imaged through separate photomultipliers by LSCM, regardless of whether Cy5- SCP-2 (Fig. 8A) or Cy5-pro-SCP-2 (Fig. 8C) were incorporated into the cells, cholera toxin B-AF488 labeled GM_1 primarily at the cell surface. Some punctuate cholera toxin B-AF488 fluorescence appeared below the plasma membrane reflecting the known very rapid endocytic uptake of L-cells (71,72). A representative image of cells incubated with Cy5-SCP-2 and cholera toxin B-AF488 showed that some Cy5-SCP-2 colocalized with cholera toxin B-AF488 labeled GM_1 at the plasma membrane (Fig. 8B). In contrast, there was much less colocalization in cells incubated with Cy5-pro-SCP-2 and cholera toxin B-AF488 (Fig. 8D). Thus, the presence of the N-terminal presequence in pro-SCP-2 resulted in less targeting to the plasma membrane caveolae/lipid rafts-consistent with the known preferential targeting of pro-SCP-2 to peroxisomes (rev. in (39).

DISCUSSION

Although a large variety of proteins that are important in cell signaling and lipid uptake/efflux reside in PM caveolae, the mechanism whereby these proteins are targeted to caveolae are not completely clear. With regards to proteins involved in signaling, to date all are thought to directly interact with caveolin-1 through specific aa binding sequences. Each signaling protein is predicted to contain a CBD that recognizes the CSD residing in aa 80-101 of caveolin-1 (47). The CSD is not only important for signaling protein recognition, but model membrane studies indicate that a peptide comprised of the caveolin-1 scaffolding domain is sufficient for membrane interaction and membrane domain formation (68). The membrane interaction component of the scaffolding domain is mediated largely by electrostatic interactions between aa segments rich in basic aa, which interact with/recruit acidic phospholipids to form lipid rafts (68). In contrast, since the CBD interaction motifs of signaling proteins contain very few acidic and even fewer basic aa, it is unlikely that these protein-caveolin-1 interactions occur primarily via electrostatic interactions (48). Instead, the CBD of interacting signaling proteins is comprised of the recognition sequence ΦXΦXXXXΦ or ΦXXXXΦXXΦ, where Φ is an aromatic aa (Trp, Phe, or Tyr) (12,48,49). These data suggest that the relatively hydrophobic CBD must interact with a relatively non-polar region present within the CSD, possibly via the seven hydrophobic residues known to reside therein (68). An important functional feature common to almost all signaling protein/caveolin-1 interactions is that caveolin-1 association inhibits the activities of the signaling proteins while posttranslational modifications (e.g. phosphorylation) disrupt such interactions and enhance the activity of signaling proteins (47,48,68).

In contrast, the signaling and cholesterol homeostatic functions of appear codependent (73). Much less is known about specific aa sequences that target proteins involved in lipid uptake/efflux to caveolae. Of the membrane-associated proteins (SRB1, ABCA1, P-gp, caveolin-1) involved in cholesterol uptake/efflux, only two of the possible interaction pairs have been demonstrated: (i) cross-linking studies show that ABCA1 directly interacts with caveolin-1, through an as yet unresolved CBD and CSD sequences (22); (ii) caveolin-1 contains the requisite CBD sequence for interacting with the caveolin CSD (48) and homo-oligomerizes — important for caveolae formation and function in signaling and lipid transport (11,34,48,68,74–76). Of the membrane associated proteins (SRB1, ABCA1, P-gp, caveolin-1) involved in cholesterol uptake/efflux, only caveolin-1 has been shown to bind cholesterol *in vitro* (17), crosslink to photoactivatable cholesterol (31,73,77), and mediate bidirectional trafficking of cholesterol to and from caveolae (17,25,78). Phosphorylation of Ser 80 within the CSD inhibits sterol binding to caveolin-1 and stimulates cholesterol efflux from cultured cells (73). The fact that SCP-2 is a ubiquitous protein found in all mammalian tissues examined, suggests that SCP-2 interaction with the N-terminus of caveolin-1 may facilitate cholesterol efflux when interaction of caveolin-1 with the caveolin-1 CSD is disrupted. To date the specific membrane protein(s) involved in cholesterol insertion into

caveolae, translocation across caveolae, and desorption from caveolae remain to be identified.

Given that the scaffolding domain of caveolin-1 recognizes the binding domain of other caveolin-1 molecules, caveolin-1/caveolin-1 oligomerization may be involved in the docking of caveolar vesicles or caveolin-1/lipid/chaperone complexes that direct cholesterol and cholesteryl ester trafficking to/from caveolae (11,34,48,68,74,76). Although FRET and immunogold electron microscopy data from our laboratory suggest that SCP-2 is in sufficient proximity to caveolin-1 for direct interaction in several cultured cell lines, examination of the aa sequence indicates that this cholesterol binding/transport protein does not contain the consensus CBD necessary for interaction with the CSD (50). The data presented herein provided several new insights and demonstrated for the first time a potential new caveolin-1 recognition domain, independent of the CSD motif, for interaction with proteins not containing the classic CBD domain.

Our previous data show full-length SCP-2 and full-length caveolin-1 interact in an *in vivo* yeast two hybrid assay. This reactivity was further shown by FRET and co-immunoprecipitation strategies, strongly suggesting a direct protein-protein interaction between these molecules (50). Therefore we evaluated the interaction of caveolin-1 mutants with SCP-2 to determine if SCP-2 bound a specific caveolin-1 domain. Reactivity of purified caveolin-1 synthetic peptides and purified SCP-2 in an *in vitro* binding assay verified a direct protein-protein interaction. However, we recognize other molecules may be involved *in vivo*. Data from the current investigation revealed the following:

First, studies with caveolin-1 mutants in the yeast two-hybrid assays demonstrated that the SCP-2 binding domain was present in the caveolin-1 N-terminal region of both α- and β-caveolin-1 isoforms.

Second, deletion of the α-caveolin-1 N-terminal aa 1-59 abolished binding to the SCP-2_{1-32}-bound beads. Conversely, the N-terminal α-caveolin-1 peptide (Cav_{2-31}) bound to sepharose beads failed to bind purified SCP-2, whereas SCP-2 bound two caveolin-1 peptides, Cav_{19-40} and Cav $_{34-55}$ with the more N-terminal peptide showing stronger reactivity. Taken together, this positive reactivity with Cav_{19-40} and Cav_{34-55}, and negative reactivity with Cav_{2-31} indicated that the SCP-2 binding site encompassed caveolin-1 residues 34-50, a new caveolin-1 binding domain. It should be noted however, that due to alternate transcription sites the caveolin-1 gene encodes for two isoforms: α-caveolin-1 and β-caveolin-1 (79,80). These isoforms differ in that the β-caveolin-1 is missing the N-terminal 32 aa (Fig. 6). Based on the fact that the putative SCP-2 binding site for α-caveolin-1 is residues 34-40, which are also present at the N-terminus of β-caveolin-1 (Fig. 6, boxed area), it is expected that SCP-2 would interact equally well with both proteins.

Third, the C-terminal deletion mutants of α-caveolin-1 1-156 and β-caveolin-1 1-156 interacted with SCP-2_{1-32} and Pro-SCP-2_{1-20} by the *in vitro* peptide binding technique, but only weakly bound full-length β-caveolin-1. These data indicate: (i) deletion of the β-caveolin-1 C-terminus facilitates exposure of the β-caveolin-1 N-terminus to interact with SCP-2; (ii) the α- caveolin-1 C-terminus is not essential to SCP-2 binding; and (iii) the caveolin-1 C-terminus influences the exposure of the caveolin-1 N-terminus. This could explain earlier results in which the rotavirus protein NSP4 interacts with both termini of caveolin-1 (54). In this study, the N-terminus of caveolin-1 was more reactive in the peptide binding assay tan the C-terminus of caveolin-1, perhaps because the role of NSP4 binding to the C-terminus of caveolin-1 is to expose the N-terminus of caveolin-1 to NSP4 for binding. Additional data are needed to verify this hypothesis, although these data are consistent with the mutant caveolin-1 SCP-2 binding results.

Fourth, deletion mutants of caveolin-1 missing all or part of the scaffolding domain (aa 80-100) interacted with SCP-2 in the yeast two-hybrid assay (CavΔ60-100 and CavΔ83-123). These data were consistent with SCP-2 lacking the aromatic consensus CBD (50). Thus, SCP-2 interaction with caveolin-1 must be mediated through a domain outside of the caveolin-1 CBD. Our laboratory showed earlier that the SCP-2 N-terminal aa1-32 has an amphipathic α-helix structure and one face of this helix is enriched with basic residues that interact with anionic phospholipids in membranes (52,63). Since both the SCP-2 N-terminus (63) and the CSD domain (68) are rich in basic aa (positively charged), this may actually result in an electrostatic repulsion between them and explain in part why SCP-2 does not bind to the CSD.

Fifth, the N-terminal aa 1-32 of SCP-2 were sufficient to provide an interaction domain for caveolin-1. The *in vitro* binding assay showed that the N-terminal peptide SCP-2_{1-32}, coupled to sepharose beads captured full-length α-caveolin-1 from lysates of MDCK cells or yeast expressing caveolin-1, but not yeast deficient in caveolin-1. SCP-2_{1-32}-sepharose beads did not capture full-length β-caveolin-1 from MDCK cell lysates. Although the current findings demonstrate that N-terminal SCP-2_{1-32} interacts directly with the N-terminal binding site present in α-caveolin-1, it must be noted that the N-terminal SCP-2_{1-32} also represents the interaction domain with anionic phospholipids of model membranes (63,64). Circular dichroism (63,64), NMR, and crystallography studies show that SCP-2_{1-32} is comprised of an amphipathic α-helix with hydrophobic residues facing inward into a hydrophobic tunnel (38,81,82). The cationic residues face outward for interaction with membranes containing anionic phospholipids (63) or potentially proteins with patches of anionic residues (38,81,82). Caveolin-1 contains a putative α-helical domain at residues 30-40 (78). Modeling studies indicate this region could interact with the α-helical region of N-terminal SCP-2 (Table I). To disrupt the amphipathic α-helix of SCP-2_{1-32}, Leu20 (L20) was replaced with Glu20 (E20). This change results in the loss of binding to anionic phospholipids (63,64) as well as to loss of both phospholipid and cholesterol transport (70). However, as shown herein SCP-$2_{1-32E20}$ Still interacted with full length α-caveolin-1, suggesting that the interaction of SCP-2 with caveolin-1 was independent of its ability to bind/transfer cholesterol and phospholipid.

To date very little is known regarding the functional significance of these two isoforms of caveolin-1 (79). Immunofluorescence and immunogold labeling reveal that the α- and β-caveolin-1 have distinct, but overlapping distributions at the plasma membrane (80). Based on the finding that α-caveolin-1 is localized in deep caveolae while β-caveolin-1 is localized in shallower caveolae, it has been suggested that α-caveolin-1 may have greater potential to form caveolae (79). The current investigation extends the potential functional significance of these isoforms by demonstrating that only the full length α-caveolin-1, but not the β-caveolin-1, interacted with SCP-2 and the N-terminal SCP-2_{1-32}. To our knowledge this is the first report identifying a new protein binding site in α-caveolin-1 isoform at the N-terminal cytoplasmic region distinct from the scaffolding domain for a cellular protein, and the second report of a protein binding outside the CBD/CSD (54).

It is of interest to note that the 20 aa presequence present in pro-SCP-2 also interacted with the N-terminal region of caveolin-1. This N-terminal presequence is flexibly disordered in solution (83,84) suggesting that the pre-sequence may be available for interaction with caveolin-1. However, this interaction is not physiologically significant because: (i) Western blotting detects only the mature 13 kDa SCP-2, not the 15 kDa pro-SCP-2 in all mammalian tissues examined as well as in all transfected cells overexpressing pro-SCP-2 examined (rev. in (39); (ii) as shown in the present work, pro-SCP-2 bound nearly 12-fold better than SCP-2 to PEX5C, the receptor for the C-terminal peroxisomal targeting sequence-1 present in both pro-SCP-2 and SCP-2. The higher affinity of PEX5C for pro-SCP-2 vs SCP-2 was recently

confirmed by isothermal titration calorimetry (83). The enhanced affinity of the pro-SCP-2 for PEX5C is associated with greater aqueous exposure of the C-terminal peroxisomal targeting sequence-1 in pro-SCP-2 as compared to SCP-2 (60); (iii) the data presented herein show that, as compared to SCP-2, incorporation of pro-SCP-2 into cells resulted in less localization to GM_1, a marker for caveolae/lipid rafts at the plasma membrane. Photoactivatable GM_1 cross-links to caveolin-1 at the plasma membrane (85); (iv) expressing the cDNA for pro-SCP-2 in transfected cells resulted in several-fold enhanced peroxisomal targeting as compared to expression of the cDNA encoding SCP-2 (rev. in (39); (v) in normal tissues the highest concentration of SCP-2 is found in peroxisomes (rev. in (39,86); (vi) in all normal tissues and transfected cells overexpressing pro-SCP-2, the 20 aa presequence undergoes complete posttranslational cleavage at the peroxisome followed by degradation (rev. in (39); (vii) there is little difference in localization of immunoreactive SCP-2 at the plasma membrane of cells overexpressing SCP-2 or pro-SCP-2 (50,87). Thus, interaction of the 20 aa presequence with caveolin-1 in is not likely to be of functional significance since the pro-SCP-2 protein is not detectable.

The SCP-2 interaction with the N-terminal aa 34-40 of caveolin-1 is important in cholesterol trafficking: (i) The SCP-2 -N-terminal caveolin-1 interaction was highly selective for the α-caveolin-1, an isoform localized in ‘deep’ caveolae (79)—possibly representing more mature caveolae containing a fuller complement of proteins involved in reverse cholesterol transport (RCT); (ii) The binding site in α-caveolin-1 may provide a ‘docking’ area for SCP-2 to influence the activity of caveolin-1 in cholesterol transport as both SCP-2 and caveolin-1 bind cholesterol. Furthermore, the N-terminal binding site of α-caveolin-1 may optimally position SCP-2 to act either as a cholesterol donor to or a cholesterol acceptor to/from caveolin-1 or other proteins that interact with caveolin-1 within the caveolar membrane. For example, cross-linking studies show that caveolin-1 does not directly interact with SRB1 or HDL, but instead cross-links with ABCA1 which in turn cross-links with HDL (22). Taken together with the data presented herein this suggests that SCP-2 transports bound ligand (e.g. cholesterol) from intracellular sites, followed by interaction with caveolin-1 at the plasma membrane for cholesterol efflux via ABCA1 bound to HDL or apoA1. Alternately, SCP-2 bound to α-caveolin-1 in plasma membrane caveolae may function as a cholesterol acceptor from HDL tethered to ABCA1 or SRB1 localized in caveolae. These possibilities were differentiated by studies with transfected cells overexpressing SCP-2, which support the latter possibility since these cells exhibited enhanced cholesterol uptake (44), increased cholesterol transport from the plasma membrane to endoplasmic reticulum for esterification (45,88,89) and reduced efflux of cholesterol from lipid storage droplets (33). These studies with cultured cells are further supported by findings with gene targeted mice. In control-fed mice, SCP-2 overexpression induced hepatic cholesterol (unesterified and esterified) accumulation and potentiated the effect of a cholesterol-rich diet to further enhance hepatic cholesterol accumulation (90). In contrast, SCP-2/SCP-x gene ablation reduced hepatic cholesterol (especially cholesteryl ester) accumulation (46). Taken together, these data suggest that SCP-2 interaction with caveolin-1 may facilitate cholesterol desorption from caveolae for uptake or retention into the cell rather than for efflux.

Recent reports suggest additional functional significance of SCP-2 interaction with the N-terminus of α-caveolin-1 in lipid signaling. Lipid rafts/caveolae are enriched not only in cholesterol, but also in lipids involved in intracellular signaling [phosphatidylinositol (Ptdlns), phosphatidylinositol-4-phosphate (Ptdlns-4-P), phosphatidylinositol-4,5-bisphosphate (Ptdlns-4,5-P), sphingolipids, gangliosides, ceramide, and diacylglycerol] (47,51,78,91–93). SCP-2 binds and enhances transfer not only of cholesterol, but also PI and sphingolipids (35,39,94,95). SCP-2 overexpression redistributes PI from intracellular sites to plasma membrane caveolae/lipid rafts (4,51,96,97), redistributes select sphingolipid

signaling lipids to caveolae/lipid rafts (97,98), stimulates insulin mediated inositol-triphosphate production (94), and enhances conversion of ceramide to galactosyl-ceramide (95). By binding and transferring both signaling lipids such as PI, polyphosphoinositides and sphingolipids, SCP-2 interaction with caveolin-1 at PM caveolae may regulate signaling within the cell (rev. in (95,97).

In summary, the data presented herein using the yeast-two hybrid system, an *in vitro* binding assay and FRET demonstrated for the first time that SCP-2, specifically the N-terminal aa1-32 amphipathic α-helix, interacted with caveolin-1 at a site distinct from the C-terminal caveolin-1 scaffolding domain. Instead, SCP-2 bound caveolin-1 through a new domain identified in the α-caveolin-1 N-terminus between aa34-40. Disruption of the SCP-2 N-terminal amphipathic helical region (i.e. SCP-$2_{1\text{-}32E20}$) abolished binding to anionic phospholipids (63,64) and lipid transfer activity (70), but did not inhibit SCP-2 binding to α-caveolin-1 N-terminus. This indicated that ligand binding to SCP-2 and SCP-2 interaction with caveolin-1 were independent. While the 20 aa presequence present in pro-SCP-2 also interacts with α-caveolin-1, the physiological significance of this interaction is doubtful since: (i) pro-SCP-2 is much more weakly targeted to GM_1 located in plasma membrane caveolae/lipid rafts, (ii) pro-SCP-2 has 12-fold weaker affinity than SCP-2 for the peroxisomal receptor of the peroxisomal targeting sequence; (iii) pro-SCP-2 is much more highly targeted than SCP-2 to peroxisomes where the N-terminal 20 aa are cleaved such that Western blotting detects only the mature SCP-2. Finally, a more prominent interaction between SCP-2 and β-caveolin-1 was observed when the C-terminus of caveolin-1 was deleted. Since α-caveolin-1 is localized primarily in deep caveolae, these findings report one of the first structurally and potentially functionally selective interactions of a soluble lipid carrier with a specific caveolin-1 isoform.

Abbreviations

aa	amino acids
Cav1	full-length caveolin
Caveolin-1-156	C-terminal deletion mutant of caveolin-1 missing most of C-terminal cytoplasmic domain
Cav 60-178	N-terminal deletion mutant of caveolin-1 missing almost all of the N-terminal cytoplasmic domain except for the signature domain
Cav Δ83-123	caveolin-1 deletion mutant missing part of the caveolin-1 scaffolding domain and part of the transmembrane domain
Cav Δ59-100	caveolin-1 deletion mutant missing all of the scaffolding domain and signature domain
SCP-2	sterol carrier protein-2
SR-B1	scavenger receptor B1
ABC-A1	ATP-binding cassette protein A1
Pgp	P-glycoprotein
HDL	high density lipoprotein
LDL	low density lipoprotein
CSD	caveolin-1 scaffolding domain
CBD	caveolin-1 binding domain

L-FABP	liver fatty acid binding protein
CSM	complete synthetic media
CPRG	chlorophenol red β-D-galactopyranoside assay
5FOA	5-fluoroacetic acid
Ura	uracil
PI	phosphoinositol
Ptdlns	phosphatidylinositol
Ptdlns-4-P	phosphatidylinositol-4-phosphate
Ptdlns-4,5-P	phosphatidylinositol-4,5-bisphosphate
M_r	molecular weight

REFERENCES

1. Schroeder, F.; Nemecz, G. Transmembrane Cholesterol Distribution. In: Esfahami, M.; Swaney, J., editors. Advances in Cholesterol Research. Caldwell, NJ: Telford Press; 1990. p. 47-87.
2. Schroeder F, Frolov AA, Murphy EJ, Atshaves BP, Jefferson JR, Pu L, Wood WG, Foxworth WB, Kier AB. Recent advances in membrane cholesterol domain dynamics and intracellular cholesterol trafficking. Proc. Soc. Exp. Biol. Med. 1996; 213:150–177. [PubMed: 8931661]
3. Schroeder F, Gallegos AM, Atshaves BP, Storey SM, Mcintosh A, Petrescu AD, Huang H, Starodub O, Chao H, Yang H, Frolov A, Kier AB. Recent advances in membrane cholesterol microdomains: rafts, caveolae, and intracellular cholesterol trafficking. Experimental Biology and Medicine. 2001; 226:873–890. [PubMed: 11682693]
4. Schroeder, F.; Atshaves, BP.; Gallegos, AM.; Mcintosh, AL.; Liu, JC.; Kier, AB.; Huang, H.; Ball, JM. Lipid rafts and caveolae organization. In: Frank, PG.; Lisanti, MP., editors. Advances in Molecular and Cell Biology. Amsterdam: Elsevier; 2005. p. 3-36.
5. Schroeder R, London E, Brown D. Interactions between saturated acyl chains confer detergent resistance on lipids and glycosylphosphatidylinositol (GPI)-anchored proteins: GPI-anchored proteins in liposomes and cells show similar behavior. Proc. Natl. Acad. Sci. 1994; 91:12130–12134. [PubMed: 7991596]
6. Gallegos AM, Mcintosh AL, Atshaves BP, Schroeder F. Structure and cholesterol domain dynamics of an enriched caveolae/raft isolate. Biochem. J. 2004; 382:451–461. [PubMed: 15149285]
7. Gallegos AM, Storey SM, Kier AB, Schroeder F, Ball JM. Stucture and cholesterol dynamics of caveolae/raft and nonraft plasma membrane domains. Biochem. 2006; 45:12100–12116. [PubMed: 17002310]
8. Bretscher MS, Munro S. Cholesterol and the Golgi apparatus. Science. 1993; 261:1280–1281. [PubMed: 8362242]
9. Hommelgaard AM, Roepstorff K, Vilhardt F, Torgersen ML, Sandvig K, van Deurs B. Caveolae: Stable membrane domains with a potential for internalization. Traffic. 2005; 6:720–724. [PubMed: 16101676]
10. Tagawa A, Mezzacasca A, Hayer A, Longatti A, Pelkmans L, Helenius A. Assembly and trafficking of caveolar domains in the cell: caveolae as stable, cargo triggered, vesicular transporters. J. Cell Biol. 2005; 170:769–779. [PubMed: 16129785]
11. Stralfors, P. Insulin Signaling and Caveolae. In: Lisanti, MP.; Frank, PG., editors. Caveolae and Lipid Rafts: Roles in Signal Transduction and Human Disease. San Diego: Elsevier Academic Press; 2005. p. 141-169.
12. Liu P, Rudick M, Anderson RGW. Multiple functions of caveolin-1. J. Biol. Chem. 2002; 277:41295–41298. [PubMed: 12189159]
13. Brown MS, Goldstein JL. A receptor-mediated pathway for cholesterol homeostasis. [Review]. Science. 1986; 232:34–47. [PubMed: 3513311]

14. Fielding CJ, Fielding PE. Cholesterol and caveolae: structural and functional relationships. Biochimica. et. Biophysica. Acta. 2000; 1529:210–222. [PubMed: 11111090]
15. Connelly MA, Williams DL. Scavenger receptor B1: A scavenger receptor with a mission to transport high density lipoprotein lipids. Cur. Opin. Lipidology. 2004; 15:287–295.
16. Van Eck M, Pennings M, Hoekstra M, Out R, Van Berkel TJC. Scavenger receptor B1 and ATP-binding cassette transporter A1 in reverse cholesterol transport and atherosclerosis. Cur. Opin. Lipidology. 2005; 16:307–315.
17. Everson, WV.; Smart, EJ. Caveolae and the regulation of cellular cholesterol homeostasis. In: Lisanti, MP.; Frank, PG., editors. Caveolae and Lipid Rafts: Roles in Signal Transduction and the Pathogenesis of Human Disease. San Diego: Elsevier Academic Press; 2005. p. 37-55.
18. Fielding CJ, Fielding PE. Molecular physiology of reverse cholesterol transport. [Review]. J. Lipid Res. 1995; 36:211–228. [PubMed: 7751809]
19. Mendez AJ, Lin G, Wade DP, Lawn RM, Oram JF. Membrane lipid domains distinct from cholesterol/sphingomyelin-rich rafts are involved in the ABCA1-mediated lipid secretory pathway. J. Biol. Chem. 2001; 276:3158–3166. [PubMed: 11073951]
20. Oram JF, Lawn RM. ABCA1: the gatekeeper for eliminating excess tissue cholesterol. J. Lipid Res. 2001; 42:1173–1179. [PubMed: 11483617]
21. Yancey PG, Bortnick AE, Kellner-Weibel G, de la Llera-Moya M, Phillips MC, Rothblat GH. Importance of Different Pathways of Cellular Cholesterol Efflux. Arterioscler. Thromb. Vasc. Biol. 2003; 23:712–719. [PubMed: 12615688]
22. Chao WT, Tsai S-H, Lin Y-C, Lin W-W, Yang VC. Cellular localization and interaction of ABCA1 and caveolin-1 in aortic endothelial cells after HDL incubation. Biochem. Biophys. Res. Commun. 2005; 332:743–749. [PubMed: 15907796]
23. Orso E, Broccardo C, Kaminski WE, Bottcher A, Liebisch G, Drobnik W, Gotz A, Chambenoit O, Diederich W, Langmann T, Spruss T, Luciani M-F, Rothe G, Lackner KJ, Chimini G, Schmitz G. Transport of lipids from Golgi to plasma membrane is defective in Tangier disease patients and Abc1-deficient mice. Nature Genetics. 2000; 24:192–196. [PubMed: 10655069]
24. Wang N, Silver DL, Thiele C, Tall AR. ATP-binding cassette transporter A1 (ABCA1) functions as a cholesterol efflux regulatory protein. J. Biol. Chem. 2001; 276:23742–23747. [PubMed: 11309399]
25. Fielding CJ, Fielding PE. Cellular cholesterol efflux. Biochim. Biophys. Acta. 2001; 1533:175–189. [PubMed: 11731329]
26. Jodoin J, Demeule M, Fenart L, Cecchelli R, Farmer S, Linton KJ, Higgins CF, Beliveau R. P-glycoprotein in blood-brain barrier endothelial cells: interaction and oligomerization with caveolins. J. Neurochem. 2003; 87:1010–1023. [PubMed: 14622130]
27. Ronaldson PT, Bendayan M, Gingras D, Piquette-Miller M, Bendayan R. Cellular localization and functional expression of P-glycoprotein in rat astrocyte cultures. J. Neurochem. 2004; 89:788–800. [PubMed: 15086534]
28. Radeva G, Perabo J, Sharom FJ. P-glycoprotein is localized in intermediate density membrane microdomains distinct from classical lipid rafts and caveolar domains. FEBS J. 2005; 272:4924–4937. [PubMed: 16176266]
29. Daleke DL. Phospholipid flippases. J. Biol. Chem. 2007; 282:821–825. [PubMed: 17130120]
30. Cruz JC, Thomas M, Wong E, Ohgami N, Sugii S, Curphey T, Chang CCY, Chang T-Y. Synthesis and biochemical properties of a new photoactivatable cholesterol analog 7,7-azocholestanol and its linoleate ester in Chinese hamster ovary cell lines. J. Lipid Res. 2002; 43:1341–1347. [PubMed: 12177179]
31. Thiele C, Hannah MJ, Fahrenholz F, Huttner WB. Cholesterol binds to synaptophysin and is required for biogenesis of synaptic vesicles. Nature Cell Biology. 1999; 2:42–49.
32. Frolov A, Petrescu A, Atshaves BP, So PTC, Gratton E, Serrero G, Schroeder F. High density lipoprotein mediated cholesterol uptake and targeting to lipid droplets in intact L-cell fibroblasts. J. Biol. Chem. 2000; 275:12769–12780. [PubMed: 10777574]
33. Atshaves BP, Starodub O, Mcintosh AL, Roths JB, Kier AB, Schroeder F. Sterol carrier protein-2 alters HDL-mediated cholesterol efflux. J. Biol. Chem. 2000; 275:36852–36861. [PubMed: 10954705]

34. Fielding CJ, Fielding PE. Caveolae and intracellular trafficking of cholesterol. Adv. Drug Delivery Rev. 2001; 49:251–264.
35. Schroeder, F.; Frolov, A.; Schoer, J.; Gallegos, A.; Atshaves, BP.; Stolowich, NJ.; Scott, AI.; Kier, AB. Intracellular sterol binding proteins, cholesterol transport and membrane domains. In: Chang, TY.; Freeman, DA., editors. Intracellular Cholesterol Trafficking. Boston: Kluwer Academic Publishers; 1998. p. 213-234.
36. Fuchs M, Hafer A, Muench C, Kannenberg F, Teichmann S, Scheibner J, Stange EF, Seedorf U. Disruption of the sterol carrier protein 2 gene in mice impairs biliary lipid and hepatic cholesterol metabolism. J. Biol. Chem. 2001; 276:48058–48065. [PubMed: 11673458]
37. Stolowich NJ, Frolov A, Petrescu AD, Scott AI, Billheimer JT, Schroeder F. Holo-sterol carrier protein-2: ^{13}C-NMR investigation of cholesterol and fatty acid binding sites. J. Biol. Chem. 1999; 274:35425–35433. [PubMed: 10585412]
38. Stolowich NJ, Petrescu AD, Huang H, Martin G, Scott AI, Schroeder F. Sterol carrier protein-2: structure reveals function. Cell. Mol. Life Sci. 2002; 59:193–212. [PubMed: 11915938]
39. Gallegos AM, Atshaves BP, Storey SM, Starodub O, Petrescu AD, Huang H, Mcintosh A, Martin G, Chao H, Kier AB, Schroeder F. Gene structure, intracellular localization, and functional roles of sterol carrier protein-2. Prog. Lipid Res. 2001; 40:498–563. [PubMed: 11591437]
40. Fuchs M, Lammert F, Wang DQH, Paigen B, Carey MC, Cohen DE. Sterol carrier protein-2 participates in hypersecretion of biliary cholesterol during cholesterol gallstone formation in genetically gallstone susceptible mice. Biochem. J. 1998; 336:33–37. [PubMed: 9806881]
41. Hafer A, Katzberg N, Muench C, Scheibner J, Stange EF, Seedorf U, Fuchs M. Studies with sterol carrier protein-2 (SCP-2) gene knockout mice identify liver fatty acid binding protein (FABP1) as intracellular cholesterol transporter contributing to biliary cholesterol hypersecretion and gallstone formation. Gastroenterology. 2000; 118([4, Part 1 Supplement 2]):135.
42. Martin GG, Atshaves BP, Mcintosh AL, Mackie JT, Kier AB, Schroeder F. Liver fatty acid binding protein (L-FABP) gene ablation alters liver bile acid metabolism in male mice. Biochem. J. 2005; 391:549–560. [PubMed: 15984932]
43. Martin GG, Atshaves BP, Mcintosh AL, Mackie JT, Kier AB, Schroeder F. Liver fatty acid binding protein (L-FABP) gene ablation potentiates hepatic cholesterol accumulation in cholesterol-fed female mice. Am. J. Physiol. 2006; 290:G36–G48.
44. Moncecchi DM, Murphy EJ, Prows DR, Schroeder F. Sterol carrier protein-2 expression in mouse L-cell fibroblasts alters cholesterol uptake. Biochim. Biophys. Acta. 1996; 1302:110–116. [PubMed: 8695660]
45. Murphy EJ, Schroeder F. Sterol carrier protein-2 mediated cholesterol esterification in transfected L-cell fibroblasts. Biochim. Biophys. Acta. 1997; 1345:283–292. [PubMed: 9150248]
46. Seedorf U, Raabe M, Ellinghaus P, Kannenberg F, Fobker M, Engel T, Denis S, Wouters F, Wirtz KWA, Wanders RJA, Maeda N, Assmann G. Defective peroxisomal catabolism of branched fatty acyl coenzyme A in mice lacking the sterol carrier protein-2/sterol carrier protein-x gene function. Genes and Development. 1998; 12:1189–1201. [PubMed: 9553048]
47. Smart EJ, Graf GA, McNiven MA, Sessa WC, Engelman JA, Scherer PE, Okamoto T, Lisanti MP. Caveolins, Liquid-ordered domains, and signal transduction. Mol. Cell. Biol. 1999; 19:7289–7304. [PubMed: 10523618]
48. Couet J, Li S, Okamoto M, Ikezu T, Lisanti MP. Identification of peptide and protein ligands for the caveolin-scaffolding domain. J. Biol. Chem. 1997; 272:6525–6533. [PubMed: 9045678]
49. Krajewska WM, Maslowska I. Caveolins: structure and funciton in signal transduction. Cell. Mol. Biol. Lett. 2004; 9:195–220. [PubMed: 15213803]
50. Zhou M, Parr RD, Petrescu AD, Payne HR, Atshaves BP, Kier AB, Ball JA, Schroeder F. Sterol carrier protein-2 directly interacts with caveolin-1 in vitro and in vivo. Biochem. 2004; 43:7288–7306. [PubMed: 15182174]
51. Atshaves BP, Gallegos A, Mcintosh AL, Kier AB, Schroeder F. Sterol carrier protein-2 selectively alters lipid composition and cholesterol dynamics of caveolae/lipid raft vs non-raft domains in L-cell fibroblast plasma membranes. Biochemistry. 2003; 42:14583–14598. [PubMed: 14661971]
52. Huang H, Schroeder F, Estes MK, McPherson T, Ball JM. The interactions of rotavirus NSP4 C-terminal peptides with model membranes. Biochem. J. 2004; 380:723–733. [PubMed: 15012630]

53. Parr RD, Storey SM, Mitchell DM, Mcintosh AL, Zhou M, Mir KD, Ball JM. The rotavirus enterotoxin, NSP4, directly interacts wtih the caveolae structural protein, caveolin-1. J. Virol. 2006; 80:2842–2854. [PubMed: 16501093]
54. Huang H, Starodub O, Mcintosh A, Kier AB, Schroeder F. Liver fatty acid binding protein targets fatty acids to the nucleus: real-time confocal and multiphoton fluorescence imaging in living cells. J. Biol. Chem. 2002; 277:29139–29151. [PubMed: 12023965]
55. Mir KD, Parr RD, Schroeder F, Ball JM. Virus Res. in press
56. Gietz RD, Woods RA. Transformation of yeast by lithium acetate/single-stranded carrier DNA/polyethylene glycol method. Methods in Enzymology. 2002; 350:87–96. [PubMed: 12073338]
57. Landy A. Dynamic, structural, and regulatory aspects of lambda-site-specific recombination. Annu. Rev. Biochem. 1989; 58:913–949. [PubMed: 2528323]
58. Vidal, M. The reverse two-hybrid system. In: Bartel, P.; Fields, S., editors. The Two-hybrid System. New York: Oxford University Press; 1997. p. 109
59. Vidal M, Brachman RK, Fattaey A, Harlow E, Boeke JD. Reverse two-hybrid and one-hybrid systems to detect dissociation of protein-protein and DNA-protein interactions. Proc. Natl. Acad. Sci. 1996; 93:10315–10320. [PubMed: 8816797]
60. Schroeder F, Frolov A, Starodub O, Russell W, Atshaves BP, Petrescu AD, Huang H, Gallegos A, Mcintosh A, Tahotna D, Russell D, Billheimer JT, Baum CL, Kier AB. Pro-sterol carrier protein-2: role of the N-terminal presequence in structure, function, and peroxisomal targeting. J. Biol. Chem. 2000; 275:25547–25555. [PubMed: 10833510]
61. Yamamoto R, Kallen CB, Babalola GO, Rennert H, Billheimer JT, Strauss JFI. Cloning and expression of a cDNA encoding human sterol carrier protein 2. Proc. Natl. Acad. Sci. 1991; 88:463–467. [PubMed: 1703300]
62. Billheimer JT, Strehl LL, Davis GL, Strauss III JF, Davis LG. Characterization of a cDNA encoding rat sterol carrier protein-$_2$. DNA Cell Biol. 1990; 9:159–165. [PubMed: 2340090]
63. Huang H, Ball JA, Billheimer JT, Schroeder F. The sterol carrier protein-2 amino terminus: a membrane interaction domain. Biochemistry. 1999; 38:13231–13243. [PubMed: 10529196]
64. Huang H, Ball JA, Billheimer JT, Schroeder F. Interaction of the N-terminus of sterol carrier protein-2 with membranes: role of membrane curvature. Biochem. J. 1999; 344:593–603. [PubMed: 10567245]
65. Huang H, Gallegos A, Zhou M, Ball JM, Schroeder F. Role of sterol carrier protein-2 N-terminal membrane binding domain in sterol transfer. Biochemistry. 2002; 41:12149–12162. [PubMed: 12356316]
66. Hostetler HA, Petrescu AD, Kier AB, Schroeder F. Peroxisome proliferator activated receptor alpha (PPARalpha) interacts with high affinity and is conformationally responsive to endogenous ligands. J. Biol. Chem. 2005; 280:18667–18682. [PubMed: 15774422]
67. Petrescu AD, Payne HR, Boedeker AL, Chao H, Hertz R, Bar-Tana J, Schroeder F, Kier AB. Physical and functional interaction of acyl CoA binding protein (ACBP) with hepatocyte nuclear factor-4alpha (HNF4alpha). J. Biol. Chem. 2003; 278:51813–51824. [PubMed: 14530276]
68. Wanaski S, Ng BK, Glaser M. Caveolin scaffolding region and the membrane binding region of Src form lateral membrane domains. Biochem. 2003; 42:42–46. [PubMed: 12515538]
69. Ikonen E, Heino S, Lusa S. Caveolins and membrane cholesterol. Biochem. Soc. Trans. 2004; 32:121–123. [PubMed: 14748728]
70. Seedorf U, Scheek S, Engel T, Steif C, Hinz HJ, Assmann G. Structure-activity studies of human sterol carrier protein 2. J. Biol. Chem. 1994; 269:2613–2618. [PubMed: 8300590]
71. Schroeder F, Kier AB. Lipid composition alters phagocytosis of fluorescent latex beads. J. Immunol. Methods. 1983; 57:363–371. [PubMed: 6827111]
72. Schroeder F, Kinden DA. Measurement of phagocytosis using fluorescent latex beads. J. Biochem. Biophys. Meth. 1983; 8:15–27. [PubMed: 6630865]
73. Fielding PE, Chau P, Liu D, Spencer TA, Fielding CJ. Mechanism of platelet derived growth factor dependent caveolin-1 phosphorylation: relationship to sterol binding and the role of serine-80. Biochem. 2004; 43:2578–2586. [PubMed: 14992595]

74. Feron, O. The Caveolin Interaction with Endothelial Nitric Oxide Synthase (eNOS). In: Lisanti, MP.; Frank, PG., editors. Caveolae and Lipid Rafts: Roles in Signal Transduction and the Pathogenesis of Human Disease. San Diego: Elsevier Academic Press; 2005. p. 91-108.
75. Monier S, Dietzen DJ, Hastings WR, Lublin DM, Kurzchalia TV. Oligomerization of VIP21-caveolin in vitro is stabilized by long chain fatty acylation or cholesterol. FEBS Lts. 1996; 388:143–149.
76. Igarashi K, Kaneda M, Yamaji A, Saido TC, Kikkawa U, Ono Y, Inoue K, Umeda M. A novel phosphatidylserine-binding peptide motif defined by an anti-idiotype monoclonal antibody. Localization of phosphatidylserine-specific binding sites on protein kinase C and phosphatidylserine decarboxylase. J. Biol. Chem. 1995; 270:29075–29078. [PubMed: 7493929]
77. Fielding PE, Russell JS, Spencer TA, Hakamata H, Nagao K, Fielding CJ. Sterol efflux to apolipprotein A-1 originates from caveolin-rich microdomains and potentiates PDGF-dependent protein kinase activity. Biochem. 2002; 41:4929–4937. [PubMed: 11939788]
78. Smart, EJ.; van der Westhuyzen, DR. Scavenger receptors, caveolae, caveolin, and cholesterol trafficking. In: Chang, TY.; Freeman, DA., editors. Intracellular Cholesterol Trafficking. Boston: Kluwer Academic Publishers; 1998. p. 253-272.
79. Fujimoto T, Kogo H, Nomura R, Une T. Isoforms of caveolin-1 and caveolar structure. J. Cell Sci. 2001; 113:3509–3517. [PubMed: 10984441]
80. Scherer PE, Tan Z, Chun M, Sargiacomo M, Lodish HF, Lisanti MP. Caveolin isoforms differ in their N-terminal protein sequence and subcellular distribution. J. Biol. Chem. 1995; 270:16395–16401. [PubMed: 7608210]
81. Garcia FL, Szyperski T, Dyer JH, Choinowski T, Seedorf U, Hauser H, Wuthrich K. NMR structure of the sterol carrier protein-2: implications for the biological role. J. Mol. Biol. 2000; 295:595–603. [PubMed: 10623549]
82. Choinowski T, Hauser H, Piotnek K. Structure of sterol carrier protein 2 at 1.8 A resolution reveals a hydrophobic tunnel suitable for lipid binding. Biochemistry. 2000; 39:1897–1902. [PubMed: 10684638]
83. Stanley WA, Filipp FV, Kursula P, Schuller N, Erdmann R, Schliebs W, Sattler M, Wilmanns M. Recognition of a functional peroxisome type 1 target by dynamic import receptor Pex5p. Mol. Cell. 2006; 24:653–663. [PubMed: 17157249]
84. Weber FE, Dyer JH, Garcia FL, Werder M, Szyperski T, Wuthrich K, Hauser H. In pre-sterol carrier protein 2 (SCP2) in solution the leader peptide is flexibly disordered, and residues 21-143 adopt the same globular fold as in mature SCP-2. Cell. Mol. Life Sci. 1998; 54:751–759. [PubMed: 9711242]
85. Pitto M, Brunner J, Ferraretto A, Ravasi D, Palestini P, Masserini M. Use of a photoactivatable GM1 ganglioside analogue to assess lipid distribution in caveolae bilayer. Glycoconjugate Journal. 2000; 17:215–222. [PubMed: 11201793]
86. Keller GA, Scallen TJ, Clarke D, Maher PA, Krisans SK, Singer SJ. Subcellular localization of sterol carrier protein-2 in rat hepatocytes: its primary localization to peroxisomes. J. Cell Biol. 1989; 108:1353–1361. [PubMed: 2925789]
87. Starodub O, Jolly CA, Atshaves BP, Roths JB, Murphy EJ, Kier AB, Schroeder F. Sterol carrier protein-2 immunolocalization in endoplasmic reticulum and stimulation of phospholipid formation. Am. J. Physiol. 2000; 279:C1259–C1269.
88. Frolov A, Woodford JK, Murphy EJ, Billheimer JT, Schroeder F. Spontaneous and protein-mediated sterol transfer between intracellular membranes. J. Biol. Chem. 1996; 271:16075–16083. [PubMed: 8663152]
89. Frolov AA, Woodford JK, Murphy EJ, Billheimer JT, Schroeder F. Fibroblast membrane sterol kinetic domains: modulation by sterol carrier protein 2 and liver fatty acid binding protein. J. Lipid Res. 1996; 37:1862–1874. [PubMed: 8895052]
90. Atshaves BP, Mcintosh AL, Landrock D, Payne HR, Schroeder F, Kier AB. Sterol carrier protein-2 expression in female transgenic mice potentiates diet-induced hepatic cholesterol accumulation. Lipids submitted. 2007
91. Anderson RGW. Plasmalemmal caveolae and GPI-anchored membrane proteins. Cell Biology. 1993; 5:647–652.

92. Anderson R. The caveolae membrane system. Ann. Rev. Biochem. 1998; 67:199–225. [PubMed: 9759488]

93. Waugh MG, Lawson D, Tan SK, Hsuan JJ. Phosphatidyl 4-phosphate synthesis in immunoisolated caveolae-like vesicles and low buoyant non-caveolar membranes. J. Biol. Chem. 1998; 273:17115–17121. [PubMed: 9642278]

94. Schroeder F, Zhou M, Swaggerty CL, Atshaves BP, Petrescu AD, Storey S, Martin GG, Huang H, Helmkamp GM, Ball JM. Sterol carrier protein-2 functions in phosphatidylinositol transfer and signaling. Biochemistry. 2003; 42:3189–3202. [PubMed: 12641450]

95. Milis DG, Moore MK, Atshaves BP, Schroeder F, Jefferson JR. Sterol carrier protein-2 expression alters sphingolipid metabolism in transfected mouse L-cell fibroblasts. Mol. Cell. Biochem. 2006; 283:57–66. [PubMed: 16444586]

96. Incerpi S, Jefferson JR, Wood WG, Ball WJ, Schroeder F. Na pump and plasma membrane structure in L-cell fibroblasts expressing rat liver fatty acid binding protein. Arch. Biochem. Biophys. 1992; 298:35–42. [PubMed: 1326253]

97. Schroeder F, Atshaves BP, Mcintosh AL, Gallegos AM, Storey SM, Parr RD, Jefferson JR, Ball JM, Kier AB. Sterol carrier protein-2: New roles in regulating lipid rafts and signaling. Biochim. Biophys. Acta. in press

98. Atshaves BP, Jefferson JR, Kier AB, Schroeder F. Sterol carrier protein-2, a new sphingolipid binding protein, alters sphingolipid distribution in plasma membrane caveolae/lipid raft domains. Biochemical Journal. 2007 submitted.

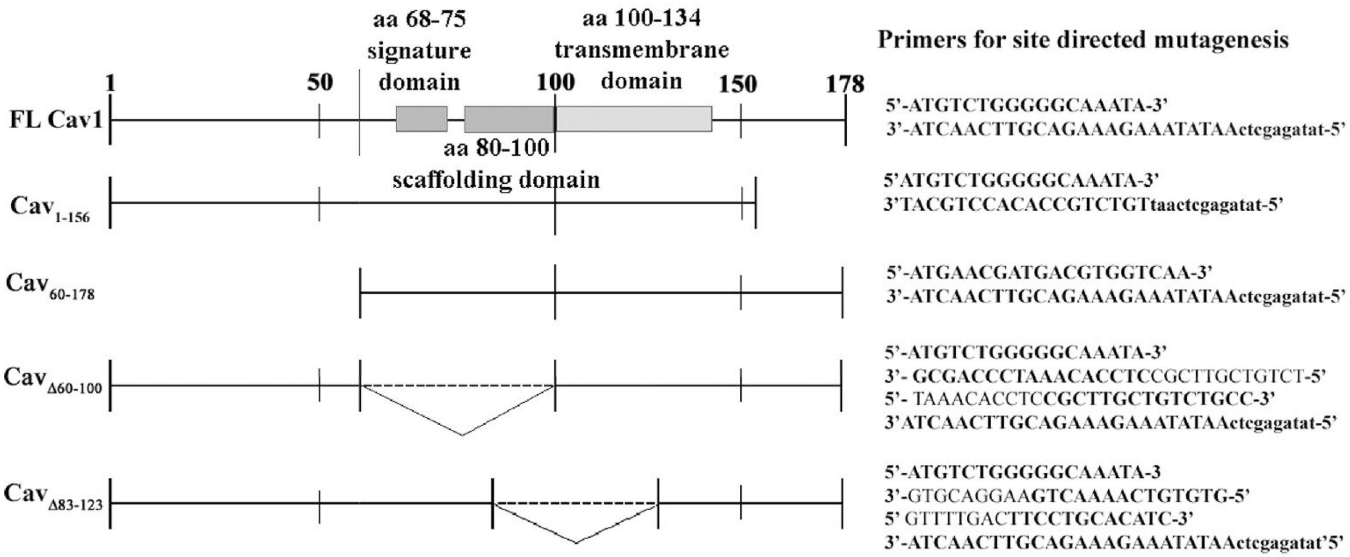

Figure 1. A linear schematic of full length and deletion mutants of caveolin-1

The PCR fragments were produced using the forward and reverse primers listed to the right of each construct and cloned into the DNA-binding domain plasmid, pD22, and the activation-domain plasmid, pD32 of the ProQuest™ Yeast two-Hybrid System with Gateway™ Technology. The full length clone of caveolin-1 encodes 178 amino acids. One 3' deletion mutant, Caveolin-1-156, one 5' deletion mutant, Cav 60-178, and two internal deletion mutants, Cav Δ60-100 and Δ83-123 were produced as described in Material and Methods

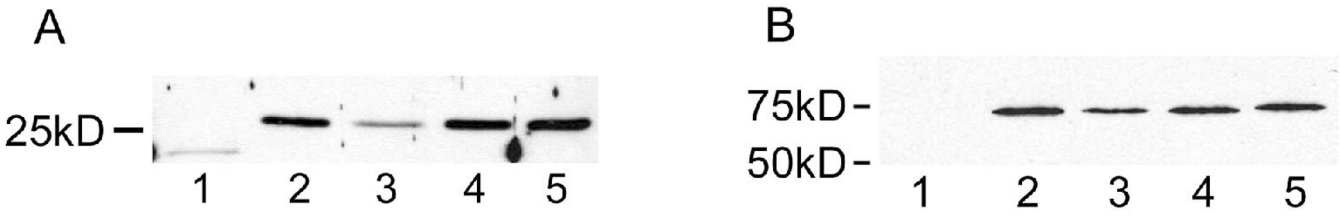

Figure 2. Expression of SCP-2- and caveolin-1- fusion proteins in co-transformed yeast

Untransfected (lanes 1) and co-transfected MaV203 yeast cell lysates containing pD32CavlΔ83-123 (lanes 2), pD32CavlΔ60-100 (lanes 3), pD32 Cav1 1-156 (lanes 4), and pD32Cav1 (lanes 5) were separated on 12% SDS-PAGE and transferred onto nitrocellulose membranes. The blots were probed with rabbit anti-SCP-2_{1-32} (panel A) or anti-Cav_{2-31} (panel B) followed by goat anti-rabbit HRP-conjugated secondary antibodies.

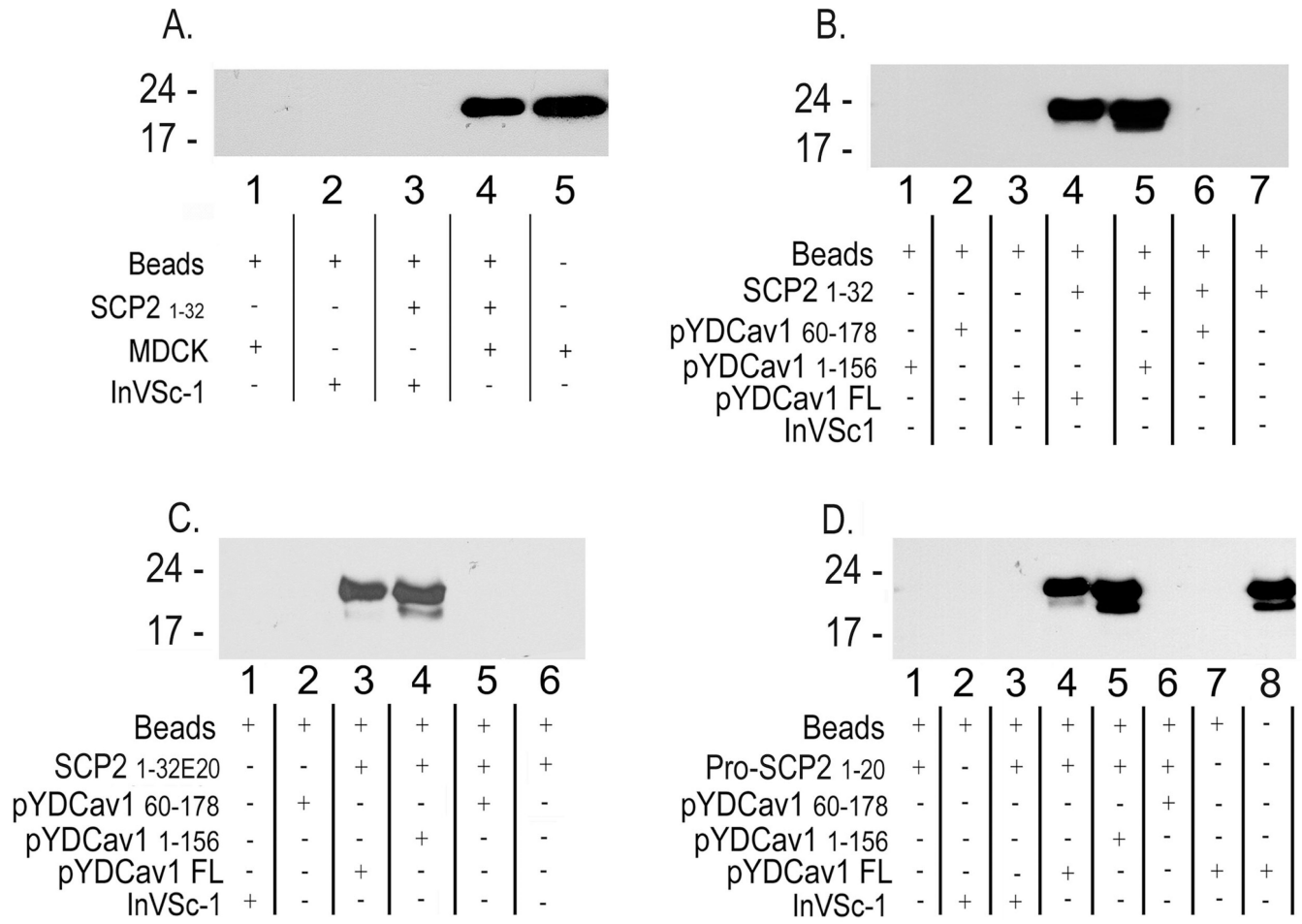

Figure 3. SCP-2_{1-32} binding assays: MDCK cell lysates and yeast expressing caveolin-1 (pY52DCav1)

MDCK or lnVSc-1 cell lysates were incubated with the immobilized SCP-2_{1-32} (sepharose-4B-SCP-2_{1-32}), separated on 12% SDS-PAGE, transferred to nitrocellulose membranes, probed with rabbit caveolin-1 antisera and detected as described in Material and Methods. Panel A. Analysis of MDCK (lane 4) and lnVsc-1 (lane 3) lysates reacted with sepharose-4B-SCP-2_{1-32}. Beads only with each of the lysates served as a negative control (lanes 1 and 2). Unreacted MDCK lysates was utilized as the positive control (lane 5). Panel B. Sepharose-4B-SCP-2_{1-32} reacted with yeast lysates expressing full length caveolin-1 (lane 4), and caveolin-1 deletion mutants, Cav1 1-156 (lane 5), Cav1 60-178 (lane 6). Each lysate was reacted with beads only (lanes 1–3) to show specificity with SCP-2_{1-32}. Lane 7 shows beads and peptide only. Panel C. Sepharose-4B-SCP-$2_{1-32E20}$. reacted with yeast lysates expressing full-length caveolin-1 (lane 3), and caveolin-1 deletion mutants, Cav1 1-156 (lane 4), Cav1 60-178 (lane 5). Beads with no peptide were reacted with lysates from either untransformed yeast (lnvSC-1) or yeast expressing Cav1 60-178 (lanes 1 and 2, respectively) to show specificity with SCP-$2_{1-32E20}$. Lane 6 shows beads and peptide only. Panel D. Sepharose-4B-pro-SCP-2_{1-20} reacted with yeast lysates expressing full-length caveolin-1 (lane 4), and caveolin-1 deletion mutants, Cav1 1-156 (lane 5), Cav1 60-178 (lane 6). Lysates were reacted with beads only (lanes 2,7) to show specificity with SCP-2_{1-32}. Lane 1 shows beads and peptide only. Lane 8 shows the specificity of the antibody for caveolin-1 expressed from full-length caveolin-1.

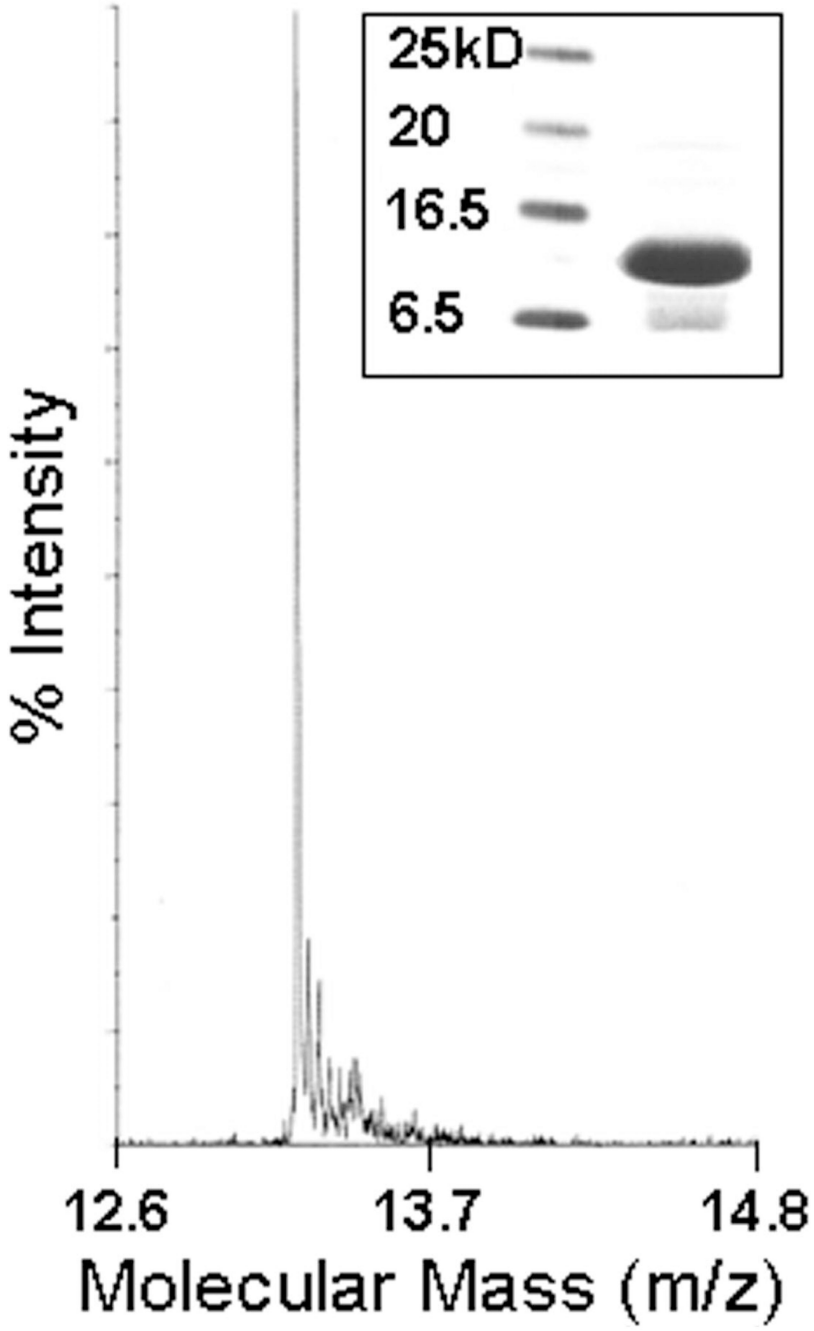

Figure 4. Mass spectrum and SDS-PAGE analysis of purified recombinant SCP-2

SCP-2 was IPTG-induced and purified from the E.coli strain, W3110, and examined by mass spectrometry and SDS-PAGE with silver stain. Matrix assisted laser desorption ionization-time of flight (MALDI-TOF) mass spectrum of SCP-2 is shown. The inset is a photograph of a silver-stained gel after SDS-PAGE of molecular size markers (lane 1) and 10 mg of SCP-2 (lane 2).

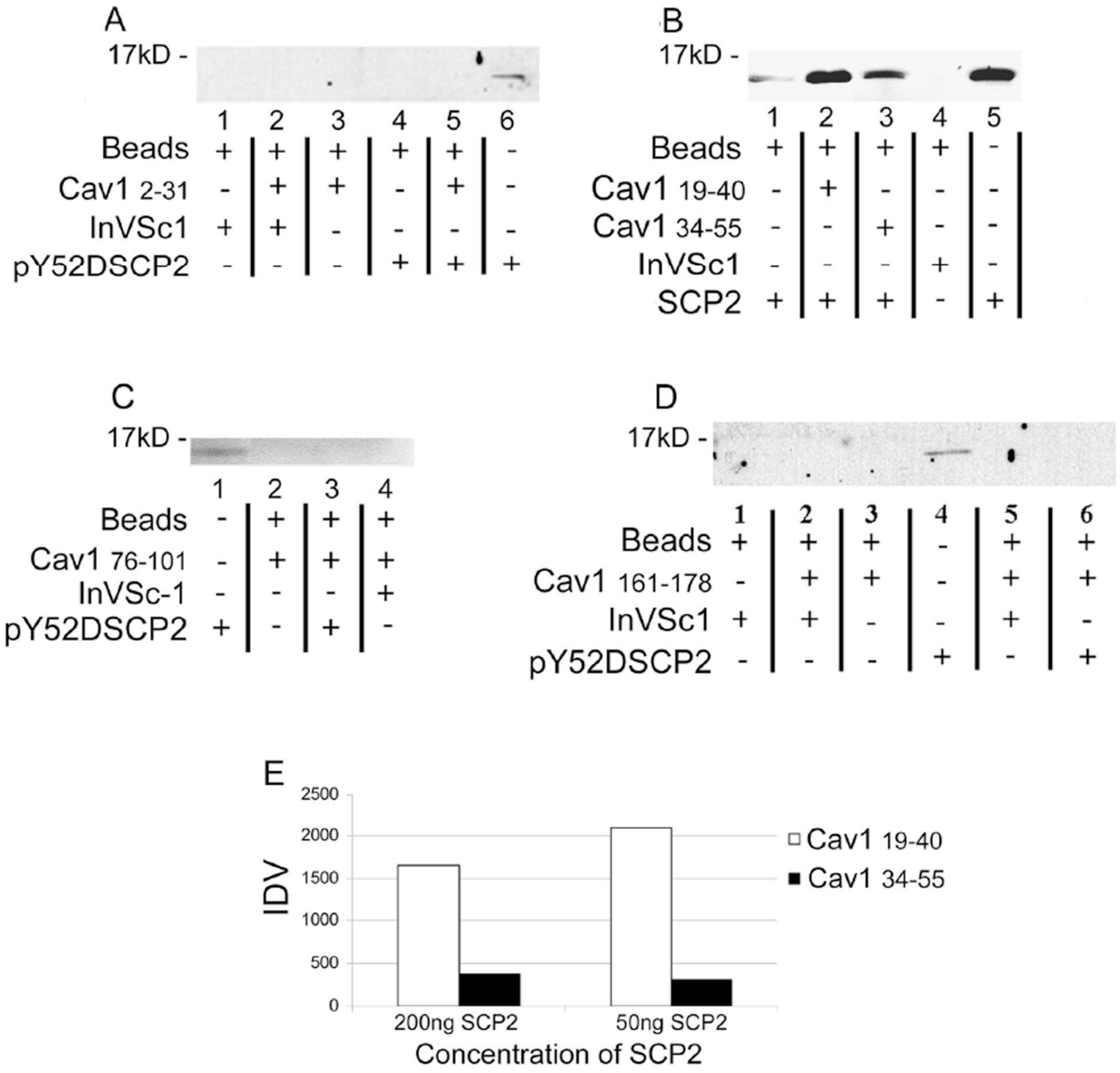

Figure 5. Absence of SCP-2 binding to mutant caveolin-1 peptides (Cav1 2-32 and Cav1 167-178) coupled to sepharose beads

Caveolin-1 synthetic peptides (aa 2-31, 19-40, 34-55, 76-101, 161-178) were linked to sepharose beads and reacted with lnVSc-1 only (negative control), yeast expressing SCP-2 (panels A, C and D) or purified recombinant SCP-2 (panel B). Peptides bound to beads were reacted with SCP-2, washed, separated on a 12% SDS-PAGE, transferred to nitrocellulose and reacted with anti-sera specific to SCP-2. Panel A. Yeast expressing SCP-2 only (lane 6) or reacted with beads only (lane 4), or beads bound by the N-terminal caveolin-1 peptide (aa 2-31, lane 5). Panel B. Purified recombinant SCP-2 (lane 5) was reacted with sepharose beads bound with $Cav1_{19-40}$ (lane 2) or $Cav1_{34-55}$ (lane 3). InVSc1 and beads only are shown in lane 4 and purified SCP-2 with unbound beads is shown in lane 1. Panels C and D. Akin to panel A, yeast expressing SCP-2 were reacted with caveolin-1 peptide-bound

sepharose beads. Panel C shows reactivity with the $Cav1_{76-101}$ (lane 3) and panel D with $Cav1_{161-178}$ (lane 6). Controls in both panels included InVSd (panel C, lane 4; panel D, lanes 2 and 5), expressed SCP-2 only (panel C, lane 1; panel D, lane 4), and beads only (no peptide) (panel D, lane 1). Panel E. Due to the low reactivity with purified SCP-2 and beads only (see panel B, lane 1), additional studies were performed using different concentrations of SCP-2 and constant concentrations of sepharose beads only or bound to peptides. These results are graphically shown in panel E. The y-axis shows the average integrated density value (IDV) equivalent to IDV/area. The x-axis shows the concentration of purified recombinant SCP-2 reacted with $Cav1_{19-40}$ (□) or $Cav1_{34-55}$ (■). The values of the average IDV acquired with SCP-2 reacted with beads only were subtracted from the average IDV of SCP-2 reacted with peptide-bound beads and therefore not shown.

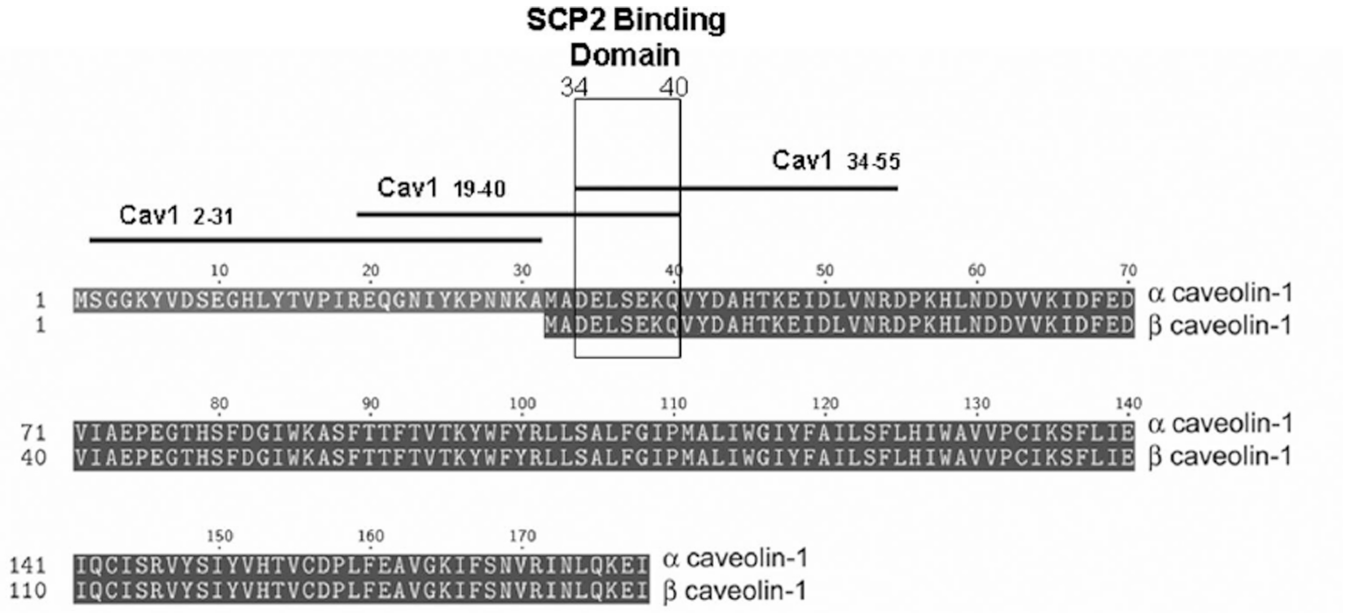

Figure 6. Sequence comparison of α- and β-caveolin-1: interaction sites with SCP-2 N-terminus

The sequences of α-caveolin-1 and β-caveolin-1 are aligned with three caveolin-1 peptides ($Cav1_{2-31}$, $Cav1_{19-40}$, and $Cav1_{34-55}$) to map the SCP-2 binding site. Full-length SCP-2 did not react with $Cav1_{2-31}$, but did react with both $Cav1_{19-40}$, and $Cav1_{34-55}$, which has an overlap of sequences from a.a. 34-40.

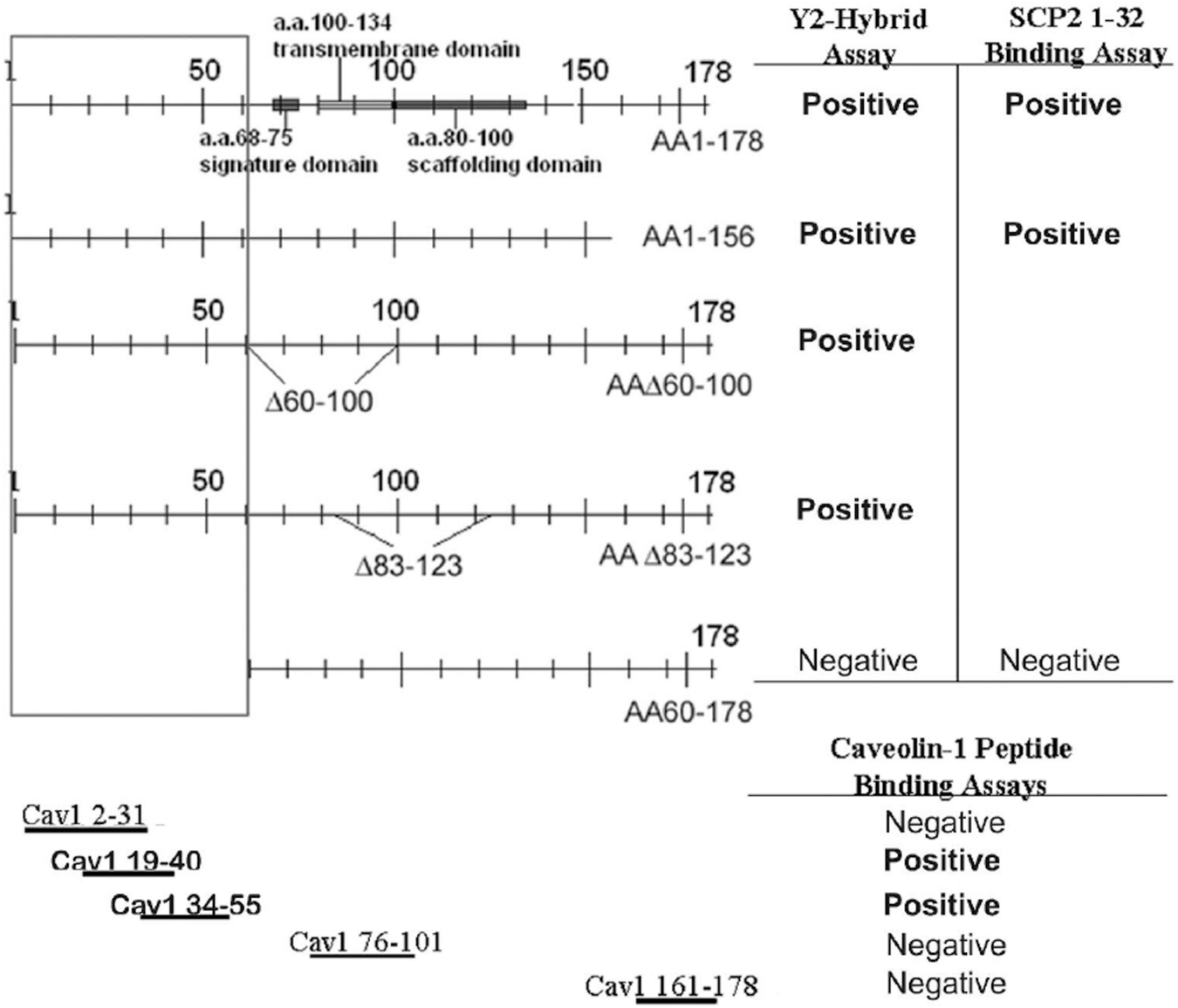

Figure 7. Summary of SCP-2 and caveolin-1 binding data

The known functional domains (signature domain aa 68-75, scaffolding domain aa 80-100, and transmembrane domain aa 100-134 of caveolin-1 are shown in the full length schematic: Deletion mutations are indicated below the full length caveolin-1. The vertical rectangle marked as residues 1–59 represents the putative binding domain of caveolin-1 to SCP-2 as defined by the results of the yeast two-hybrid assay (results on the far right). SCP-2_{1-32} peptide binding assays are shown to the right of the yeast two-hybrid data. Results of the Cav1 peptide binding assays are shown at the bottom of the figure with a linear depiction of each peptide. Based on these results, the SCP-2 binding domain of caveolin-1 has been delineated to residues 32-55 (horizontal rectangle). Taken together, the SCP-2 binding domain for caveolin-1 mapped to SCP-2 residues 1-32 and the caveolin-1 binding domain for SCP-2 has been delineated to 23 residues.

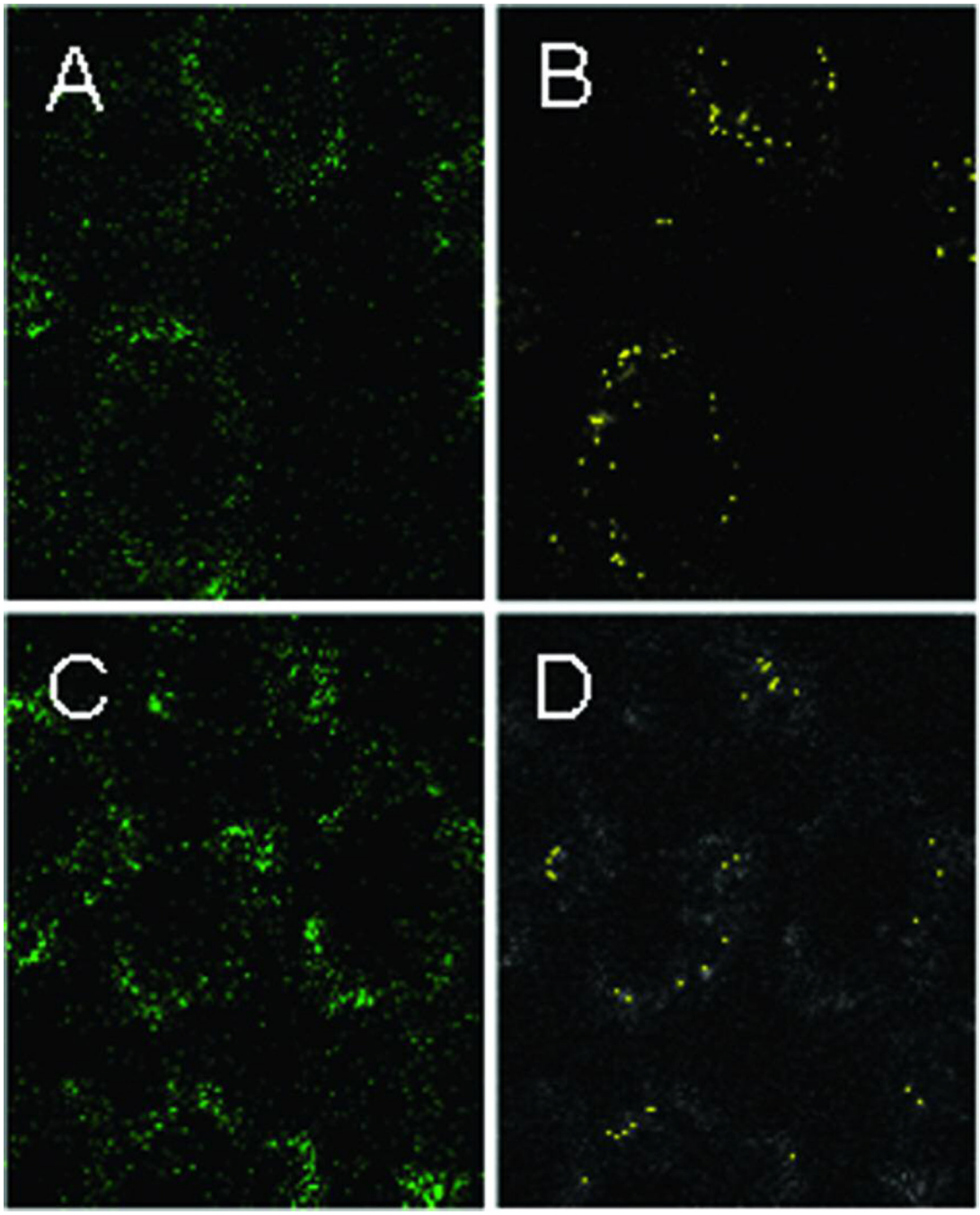

Figure 8. Colocalization of Cy5-SCP-2 or Cy5-proSCP-2 with cholera toxin B-Alexa Fluor 488 (AF488) in L cells

L cells were incubated with Cy5-labeled SCP-2 or Cy5-labeled proSCP-2, followed by Alexa Fluor 488-labeled cholera toxin B as described in Methods. Laser scanning confocal microscopic images were obtained as also as described in Methods. Panel A, cholera toxin B-AF488; panel B, Cy5-labeled SCP-2 colocalized with cholera toxin B-AF488 (yellow pixels); panel C, cholera toxin B-AF488; panel D, Cy5-labeled proSCP-2 colocalized with cholera toxin B-AF488 (yellow pixels)

Table I

Synthetic Peptide Amino acid composition and distribution

Peptides	N ⟶ C	AA distribution
Cav1 aa2-31	SGGKYVDSEGHLYTVPIREQGNIYKPNNKA	7C; 7P; 8H
Cav1 aa19-40	EQGNIYKPNNKAMADELSEKQ	7C; 6P; 4H
Cav1 aa34-55	DELSEKQVYDAHTKEIDLVNRD	11C;4P;6H
Cav1 aa76-101	EGTHSFDGIWKASFTTFTVTKYWF	4C; 9P; 7H
Cav1 aa161-178	IEKQLNIRVNSFIKGVAE	4C; 4P; 8H
SCP-2 aa1-32	SSASDGFKANLVFKEIEKKLEEEGEQFVKKIG	13C; 5P; 8H
SCP-2 aa1-32E20	SSASDGFKANLVFKEIEKKEEEEGEQFVKKIG	14C; 5P; 7H
Pro-SCP-2 aa20-0	MGFPEAASSFRTHQIEAVPT	5C; 3P; 12H

Table II

Summary of Phenotypes of Yeast Co-Transformed with pD32-Caveolin-l mutants and pD22-SCP-2

	CSM -Leu-Trp[a]	CSM -Leu-Trp− His+3AT[b]			CSM -Leu-Trp -Ura[c]	CSM -Leu-Trp + 0.2%5FOA[d]	β-gal CPRG[e]	Phenotype[f]
		12.5mM	50mM	100mM				
2+Positive	+	±	−	−	−	−	+ 5.890	**Positive**
1+Positive	+	+	+	±	±	±	± 0.202	**Positive**
Negative	+	+	±	±	−	+	− 0.072	**Negative**
Caveolin-1	+	+	−	−	−	±	± 1.755	**Positive**
Cav 1-156	+	+	−	−	−	±	+ 1.050	**Positive**
Cav 60-178	+	+	±	−	−	+	− 0.068	**Negative**
Cav Δ83-123	+	+	−	−	−	±	+ 1.243	**Positive**
Cav Δ60-100	+	−	−	−	−	±	+ 0.390	**Positive**

[a] Colonies were streaked onto complete synthetic medium lacking leucine (-Leu) & tryptophan (-Trp).

[b] Colonies were replica plated onto complete synthetic medium lacking Leu, Trp, & histidine (-His) with 12.5mM, 50mM, or 100mM 3-Amino-Triazole.

[c] Colonies were replica plated onto complete synthetic medium lacking Leu, Trp, and uracil (-Ura).

[d] Colonies were replica plated onto complete synthetic medium lacking Leu and Trp with 0.2% 5Fluorooratic acid (5FOA).

[e] Colonies were replica plated onto Yeast Peptone A Dextrose plates with nitrocellulose filters. A qualitative β-galactosidase assay was performed using X-gal, resulting in +, ±, or −. A qualitative CPRG assay was performed and reported as β-galactosidase units.

[f] Phenotype was determined by combining the results from the differential media to determine a protein-protein interaction.

Table III

Interaction of SCP-2 and pro-SCP-2 with PEX 5C[a].

FRET pair		Quenching	
Donor	**Acceptor**	**K_d(nM)**	**R(Å)**
Cy-3-PEX5C	Cy-5-SCP-2	26 ±2	66.8 ±0.8
Cy-3-PEX5C	Cy-5-Pro-SCP-2	2.3 ±0.2 *	72.4 ±0.4 *

[a] FRET was performed as described in Methods to determine binding affinity (K_d) and intermolecular distance (R).

A * refers to $p<0.05$ (n=3) vs SCP-2.